

Finite-size corrections to Fermi's golden rule : I Decay rates

Kenzo Ishikawa and Yutaka Tobita[†]

¹*Department of Physics, Faculty of Science, Hokkaido University, Sapporo 060-0810, Japan*

**E-mail: ishikawa@particle.sci.hokudai.ac.jp, tobita@particle.sci.hokudai.ac.jp*

20/3/2013

.....
A quantum mechanical wave of a finite size moves like a classical particle and shows unique decay probability. Because the wave function evolves according to a Schrödinger equation, it preserves the total energy but not the kinetic energy in the intermediate-time region of a decay process where those of the parent and daughters overlap. The decay rate computed with Fermi's golden rule requires such corrections that varies with the distance between the initial and final states, and the energy distribution of the daughter is distorted from that of plane waves. The corrections have universal properties in relativistically invariant systems and reveal macroscopic quantum phenomena for light particles. The implications to precision experiments in beta decays and various radiative transitions are presented.
.....

Subject Index B59

1. Introduction: wave zone vs particle zone

A wave length of a particle of a momentum \vec{p} is given by Planck constant \hbar as $\hbar/|\vec{p}|$, where $\hbar = h/(2\pi)$ and is of microscopic size. The momentum eigenstate is a plane wave of uniform density and many free waves of a constant kinetic-energy are also uniform in space and are like free particles. A system of many waves of varying kinetic energy shows non-uniform behavior called diffraction. A diffraction pattern has a spatial scale of the wave length normally but can become much longer in a system of a space-time symmetry. The diffraction of this kind that depends on space-time position in many-body scatterings is studied.

The diffraction gives corrections to transition probabilities computed by Fermi's golden rule. These corrections are connected with calibrations of detectors and might be known partly to experimentalists. Even so, it is important and useful to many physicists to clarify them.

In diffraction of light, electron, or others, a potential energy transforms an in-coming wave to a sum of waves of different kinetic energies. Now, a many-body interaction transforms a many-body state to a sum of the same kinetic energy, and the waves behave like free particles and do not show the diffraction at the asymptotic region, $t = \infty$. In non-asymptotic region of a finite t , however, the kinetic energy is not constant and takes broad values. So the state reveals the diffraction. Since this diffraction is caused by a many-body interaction, the

[†]This author contributed equally to this work

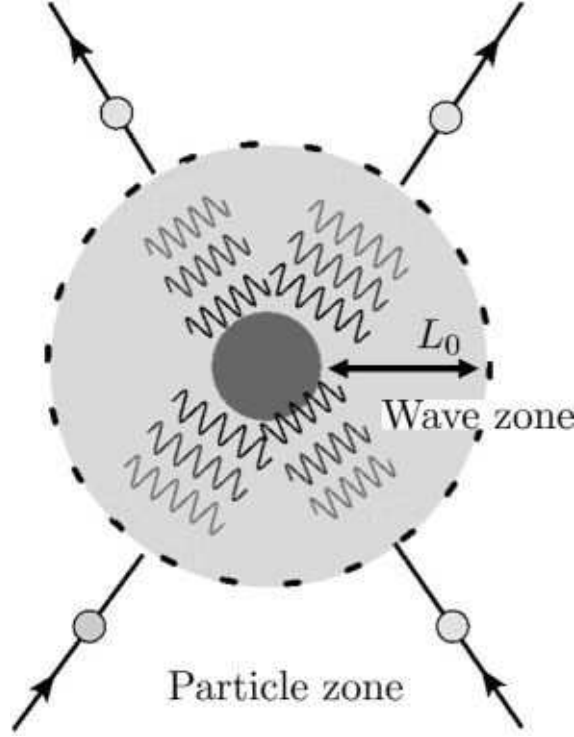


Fig. 1 In two-body scattering, in-coming particles and out-going particles in the particle-zone behave like classical particles of constant total kinetic energy but they behave like waves of non-constant kinetic energy in the wave-zone. The boundary L_0 is the coherence length and is normally a microscopic length, but becomes macroscopic in certain situation discussed in the present paper.

pattern has universal properties and appears even in vacuum. The diffraction, furthermore, gives peculiar corrections to decay rates that depend on the time interval between those of the initial and final states, which we call a finite-size correction.

Scattering processes are defined with the initial states prepared at $t = -\infty$ and the final states measured at $t = \infty$, where they do not interact with others and have no interaction energy. The initial and final states have the constant kinetic energy and reveal the particle nature. Amplitudes and probabilities in the asymptotic region have been studied well [1–5]. Now near the scattering center, the states overlap and have finite interaction energy. Thus they retain wave natures. We call the former region a particle zone, the latter region a wave zone, and a length of boundary a coherence length. Fig. (1) shows them in a two-body scattering. In the particle zone, even at a finite t , the states behave like particles. In the wave zone, however, the state reveals the wave phenomenon that depends on the position and can not be described with only the momentum dependent distribution function [6]. The coherence length has been considered microscopic in size of the order of de Broglie wave length, which may be true for most cases. Then the phenomena in the wave zone may be irrelevant to physics and unimportant. However, there has been no serious investigation on this length. We study problems connected with the wave zone and find that a new length $E\hbar/m^2$, where m and E are a particle's mass and energy, appears for the coherence length and becomes much longer than de Broglie wave length in relativistically invariant systems. A

space-time dependent phase of a relativistic wave packet $(E(\vec{p})t - \vec{p} \cdot \vec{x})/\hbar$ becomes $(E(\vec{p}) - \vec{p} \cdot \vec{v})t/\hbar = m^2 t/(\hbar E)$ of the angular velocity, $m^2/(E\hbar)$ at a position moving with the velocity, $\vec{v} = \vec{p}/E(\vec{p})$, as $\vec{x} = \vec{v}t$. The angular velocity becomes small for a light particle or at high energy and its inverse gives a new scale of length. The length becomes even macroscopic for an extremely light particle such as neutrino. Then the wave zone has a macroscopic size, and physical phenomena unique to the quantum mechanical waves occur in the macroscopic region. They are natural consequences of Schrödinger equations. The physics in this region has not been studied except for neutrino and is the subject of the present work.

Ordinarily, scattering amplitude is defined in the particle zone and is rigorously formulated with wave packets [1, 2], and in practical situations, they are approximated well with plane waves. For scattering processes at a finite-time interval, T , in the wave zone, probabilities to detect them vary with T and deviates from that of the infinite-time interval. We call the deviation a finite-size correction and we study them in various processes involving light particles in this paper.

The finite-size corrections of the scattering amplitude and probability have been considered irrelevant to experiments in high-energy regions. Plane waves with a damping factor $e^{-\epsilon|t|}$ with a positive and infinitesimal ϵ in an interaction Hamiltonian employed often for practical calculations are invariant under translations and are extended in space. This method is powerful for computing the asymptotic values but does not supply the finite-size corrections. Because the amplitude in the wave zone is sensitive to the boundary conditions of the initial and final state, that has a dependence on the distance between them. Hence, the probability has a finite-size correction which has an origin in the boundary conditions. The correction must be included for making a comparison of a theory with an experiment then. An amplitude constructed with wave packets implements manifestly the boundary conditions and supplies the finite-size correction.

Previous studies of decay processes at finite-time intervals in the particle zone using an interaction Hamiltonian of the damping factor $e^{-\epsilon|t|}$ [7–10] showed that time dependences of decay law of unstable particles are modified from simple exponential behaviors due to higher-order effects. These analysis and others of computing the decay rates are applicable to kinematical regions where the wave functions of the parent and daughters do not overlap. As was pointed out in Ref. [8] correctly, the standard method can not be applied in kinematical regions where they overlap. The states have the wave natures, and the decay rate and other physical quantities in this region have been thought neither meaningful nor computable since then. This is the region, in fact, where the probability to detect the decay product has a large finite-size correction. It is a main subject of the present work to develop a theory of S-matrix that satisfies the boundary conditions of the measuring processes and to find formulas of the physical quantities in this region. One of our results for decay rate $\Gamma(T)$ at the large distance $L = cT$, ($T < \tau$) is

$$\Gamma(T, \sigma) = \Gamma_0 + N \frac{\sigma}{T} \frac{E}{2m^2} F^2(-\tilde{m}^2), \quad \tilde{m}^2 = m_{parent}^2 - m_{daughter}^2, \quad (1)$$

where Γ_0 is the asymptotic value, τ , σ , E , m , $m_{daughter}$, and m_{parent} are the mean-life time, wave packet size, energy, and mass of the detected particle, and the mass of daughter and parent, respectively. N is a numerical constant and F is the form factor. The second term in the right-hand side of Eq. (1) is inversely proportional to T and vanishes at $T \rightarrow \infty$. So this is the finite-size correction. From its form, the correction becomes significant in small

m , large σ and E , and become macroscopic in their sizes for light particles such as photon or neutrino. This shows

$$\lim_{\sigma \rightarrow \infty} \left\{ \lim_{T \rightarrow \infty} \Gamma(T, \sigma) \right\} = \Gamma_0, \quad (2)$$

$$\lim_{T \rightarrow \infty} \left\{ \lim_{\sigma \rightarrow \infty} \Gamma(T, \sigma) \right\} = \infty. \quad (3)$$

In Eq. (2), the rate becomes the asymptotic value, whereas in Eq. (3), the rate diverges. The energy distribution reveals also unusual properties even at $T \rightarrow \infty$, if particles of large and small sizes are involved in one process. They should appear in various situations such as an interface of two phases, and interesting physics is expected. Implications on particle decays are studied.

The transition probability P composed of many processes in the particle zone are factorized to that of each microscopic process, P_i , as

$$P = \prod_i P_i. \quad (4)$$

Now, the probability for transition processes in the wave zone is not factorized due to the finite-size corrections, but the whole process is described by the product of wave functions of each microscopic process

$$\Psi = \prod_i \Psi_i, \quad P \neq \prod_i P_i. \quad (5)$$

Because the probability of the whole processes is not factorized, Markov nature of the multiple processes is lost. The non-Markov nature is related with a EPR correlation [11] and may give various implications.

The decay rates are studied in the present paper and the scattering cross sections are studied in a subsequent paper. This paper is organized in the following manner. In Section 2, a wave function and S-matrix at a finite-time interval are shown to be different from those of the infinite-time interval. Particles described by wave packets and their interactions caused by a local Hamiltonian are summarized in Section 3. Two-body decays are studied in Section 4, and radiative decays of atoms, nucleons, and particles are studied in Section 5. In Section 6 we study decay processes and thermodynamics of quantum particles. Summary is given in Section 7.

2. A finite-time interval effect

In a physical system described by a Hamiltonian H composed of a free term H_0 and an interaction term H_{int}

$$H = H_0 + H_{int}, \quad (6)$$

a wave function $|\Psi(t)\rangle$ follows the Schrödinger equation

$$i\hbar \frac{\partial}{\partial t} |\Psi(t)\rangle = (H_0 + H_{int}) |\Psi(t)\rangle. \quad (7)$$

In field theory, the free part H_0 is a bi-linear form of fields and the interaction part H_{int} is a higher polynomial of fields. H_{int} causes a change of a particle number such as a decay of a pion into a charged lepton and a neutrino.

2.1. Finite-size correction to Fermi's Golden rule

A transition rate from an eigenstate of H_0 , $|\alpha\rangle$ of energy E_α , to another $|\beta\rangle$ of energy E_β , in a wave zone at a finite-time interval T , seems to be computed with the amplitude f and probability P [12] in the form,

$$f = \int_0^T dt \langle \beta | H_{int}(t) | \alpha \rangle = \int_0^T dt e^{-i(E_\beta - E_\alpha)t} F_{\alpha,\beta}, \quad (8)$$

$$F_{\alpha,\beta} = \langle \beta | H_1(0) | \alpha \rangle,$$

$$P = |F_{\alpha,\beta}|^2 D(E_\beta - E_\alpha; T), \quad (9)$$

$$D(E_\beta - E_\alpha; T) = \frac{4 \sin^2 [(E_\beta - E_\alpha)T/2]}{(E_\beta - E_\alpha)^2},$$

where $F_{\alpha,\beta}$ is the matrix element. In a particle decay, the final state constitutes two or more particles of a continuous energy spectrum and the oscillating function $D(E_\beta - E_\alpha; T)$ approximately agrees with Dirac's delta function at the infinite T [13–15],

$$D(E_\beta - E_\alpha; T) = 2\pi T \delta(E_\beta - E_\alpha). \quad (10)$$

Because the integral of a function $F(E_\beta)$ with the weight $D(E_\beta - E_\alpha; T)$ over the energy E_β is computed with a variable $x = (E_\beta - E_\alpha)T$ as

$$\begin{aligned} P &= \int_{E_\alpha - \Delta_E}^{E_\alpha + \Delta_E} dE_\beta D(E_\beta - E_\alpha; T) F(E_\beta) \\ &= T \int_{-\Delta_E T}^{\Delta_E T} dx \left(\frac{\sin(x/2)}{x} \right)^2 F(x/T), \\ F(E_\beta) &= |F_{\alpha,\beta}|^2. \end{aligned} \quad (11)$$

The symmetric region of the integration was chosen in Eq. (11). At a large T , $F(x/T)$ is replaced with $F(0)$, and Eq. (11) becomes

$$P = TF(0) \int_{-\Delta_E T}^{\Delta_E T} dx \left(\frac{\sin(x/2)}{x} \right)^2 = 2\pi TF(0). \quad (12)$$

Thus the transition probability integrated over final states is given by

$$P = 2\pi T \int d\beta \delta(E_\alpha - E_\beta) |F_{\alpha,\beta}|^2, \quad (13)$$

and the rate P/T is constant. This is Fermi's golden rule.

Now at a finite T , expanding $F(x/T)$ in a power series of x/T

$$F(x/T) = \sum_l C_l \left(\frac{x}{T} \right)^l, \quad (14)$$

we have Eq. (11) in the form,

$$P = \sum_l C_l T^{1-l} \int_{-\Delta_E T}^{\Delta_E T} dx \left(\frac{\sin(x/2)}{x} \right)^2 x^l. \quad (15)$$

The integrals over x is easily evaluated. In a small $|x|$ region, the integrand vanishes for $l \geq 1$ and is constant for $l = 0$. In a large x region, the integrand behaves as $\frac{1}{2}x^{l-2}$. So the above

integrals become

$$\begin{aligned}
& 2\pi TC_0 + \sum_{l \geq 1} C_l T^{1-l} \int_{-\Delta_E T}^{\Delta_E T} dx \frac{x^{l-2}}{2} \\
& = 2\pi TC_0 + \sum_{l \geq 2} C_l T^{1-l} \frac{(\Delta_E T)^{l-1}}{l-1} \\
& = 2\pi TC_0 \left\{ 1 + \sum_{l \geq 2} \frac{C_l}{C_0} \frac{\Delta_E^{l-1}}{2\pi T(l-1)} \right\}. \tag{16}
\end{aligned}$$

$1/T$ correction is in the second term of the right-hand side, which is finite if Δ_E is finite. The $1/T$ correction depends on Δ_E and the distribution of eigenvalue and converges if Δ_E is finite. Appendix A and B study $1/T$ of various distributions. The value at $T \rightarrow \infty$ is defined uniquely then.

In relativistically invariant systems, $\Delta_E = \infty$ and the correction for $l \geq 2$ in Eq. (16) diverges. The infinite correction emerges due to a large overlap of wave functions in the situation where the ordinary scattering theory can not be applied [8]. The probability at a finite time measured with an apparatus does not diverge. Hence the amplitude defined according to boundary conditions of measurement process should give the finite value. The boundary condition at the finite T is different from that at the infinite T , hence the amplitude that satisfies the boundary condition at the finite T is different from those of the $T = \infty$. As is seen explicitly later, the function decreases rapidly with x/T in such manner as $e^{-\sigma(x/T)^2}$ in the right-hand side of Eq. (14), where σ is a size of wave functions determined from the boundary condition, and the coefficients converges. Since the amplitude at large x/T is determined by the boundary condition, the $1/T$ correction becomes a finite value that depends on the boundary condition. Nevertheless they follow a universal relation. It is a subject to find the universal properties of the finite-size corrections.

The states $|\beta\rangle$ of satisfying $E_\beta = E_\alpha$ contribute to the decay rate, Eq. (13) and the states $|\beta\rangle$ of $E_\beta \neq E_\alpha$ contribute to the finite-size correction. Since E_β is continuous, those states of $E_\beta \approx E_\alpha$ are sensitive to boundary conditions and so is the finite-size correction. For the computation of the probabilities of processes measured in experiments, the wave functions for the outgoing waves and in-coming waves should be localized around their centers, as were emphasized in textbooks of quantum field theory [16]. The wave packets satisfy this property and are used. They can be replaced with the plane waves in the particle zone, but in wave zone they are necessary to compute the finite-size corrections. We study the finite-size corrections to transition probabilities with wave packets. These amplitudes are described by scattering matrix $S[T]$ defined at a finite-time interval T . $S[T]$ is different from the ordinary S-matrix, $S[\infty]$, and has unique properties. The coefficients in $1/T$ expansions become finite with a use of $S[T]$.

2.2. Wave function at a finite time

$S[T]$ satisfies the boundary condition at T , and is determined by wave function which starts from an initial state at $t = 0$ and ends at a final state at $t = T$. Kinetic energy is not a good quantum number in the wave function at a finite T . A time-dependent solution of Eq. (7) in

the first order of H_{int} that satisfies a initial condition

$$|\Psi(0)\rangle = |\psi^{(0)}\rangle, \quad H_0|\psi^{(0)}\rangle = E_0|\psi^{(0)}\rangle, \quad (17)$$

is

$$|\Psi(t)\rangle = e^{-i\frac{E_0}{\hbar}t} \left\{ |\psi^{(0)}\rangle + \int d\beta d(\omega, t) |\beta\rangle \langle \beta | H_{int} | \psi^{(0)} \rangle \right\}, \quad (18)$$

$$\omega = E_\beta - E_0, \quad H_0|\beta\rangle = E_\beta|\beta\rangle,$$

where

$$d(\omega, t) = \frac{e^{-i\omega t} - 1}{\omega} = -2i \frac{\sin(\omega t/2)}{\omega} e^{-\frac{i}{2}\omega t}. \quad (19)$$

At $t \rightarrow \infty$, $d(\omega, t)$ becomes

$$d(\omega, t) = 2\pi i \delta(\omega), \quad (20)$$

and the wave function

$$|\Psi(t)_\infty\rangle = e^{-i\frac{E_0}{\hbar}t} \left\{ |\psi^{(0)}\rangle + 2\pi i |\beta\rangle \langle \beta | H_{int} | \psi^{(0)} \rangle |_{E_\beta=E_0} \right\}. \quad (21)$$

has the kinetic energy, $E_\beta \neq E_0$. At a finite t , on the other hand, Eq. (20) is not fulfilled and the wave function is a superposition of wide spectrum of the kinetic energy, E_β . An average of $d(\omega, t)$ over a finite-time interval δt of satisfying $\omega \delta t \gg 1$ is

$$d(\omega, t) = -\frac{1}{\omega}, \quad (22)$$

and the average of the wave function over the finite interval is

$$|\Psi(t)_{\text{average}}\rangle = e^{-i\frac{E_0}{\hbar}t} \left\{ |\psi^{(0)}\rangle - 2\pi i \int d\beta \frac{1}{\omega} |\beta\rangle \langle \beta | H_{int} | \psi^{(0)} \rangle |_{E_\beta=E_0} \right\}. \quad (23)$$

In both cases, the state vectors $|\Psi(t)_\infty\rangle$ and $|\Psi(t)_{\text{average}}\rangle$ have the frequency E_0/\hbar and the total energy E_0 ,

$$H|\Psi(t)_\infty\rangle = E_0|\Psi(t)_\infty\rangle, \quad (24)$$

$$H|\Psi(t)_{\text{average}}\rangle = E_0|\Psi(t)_{\text{average}}\rangle. \quad (25)$$

Thus the wave function at a finite time t is a sum of those of broad energy spectrum of H_0 , whereas that is composed of a discrete spectrum $E_\beta = E_0$ at $t = \infty$. The conservation law of energy defined with H is reduced to the conservation law of the kinetic energy defined by H_0 only at $t = \infty$.

2.3. Scattering operator at a finite-time interval

Physical quantities are observed through scattering or decay processes and are computed with $S[T]$, which is defined from unitary operators

$$U(t) = e^{-iHt}, \quad U_0 = e^{-iH_0t}. \quad (26)$$

Møller operators are defined in the form

$$\Omega_{\pm}(T) = \lim_{t \rightarrow \mp T/2} U(t)^{\dagger} U^{(0)}(t), \quad (27)$$

and satisfies

$$e^{iH\epsilon_t} \Omega_{\mp}(T) = \Omega_{\mp}(T \pm \epsilon_t) e^{iH_0\epsilon_t}. \quad (28)$$

Scattering operator at the finite time T is the product

$$S(T) = \Omega_{-}^{\dagger}(T) \Omega_{+}(T), \quad (29)$$

and satisfies

$$S(T)H_0 = H_0S(T) + i \left\{ \frac{\partial}{\partial T} \Omega_{-}(T) \right\}^{\dagger} \Omega_{+}(T) - i \Omega_{-}^{\dagger}(T) \frac{\partial}{\partial T} \Omega_{+}(T), \quad (30)$$

and the commutation relation

$$[S(T), H_0] = i \left\{ \frac{\partial}{\partial T} \Omega_{-}(T) \right\}^{\dagger} \Omega_{+}(T) - i \Omega_{-}^{\dagger}(T) \frac{\partial}{\partial T} \Omega_{+}(T). \quad (31)$$

Thus $S(T)$ does not commute with H_0 , and the conservation law of kinetic energy is violated at a finite T .

From Eq. (31), the matrix element of $S(T)$ between the eigenstates of H_0 has energy conserving and non-conserving terms,

$$\langle \beta | S(T) | \alpha \rangle = \delta_{\epsilon}(E_{\alpha} - E_{\beta}) f(T)_{\alpha, \beta} + \delta f. \quad (32)$$

where the second term, δf , vanishes at the energy $E_{\beta} = E_{\alpha}$. Since the energy E_{β} of the first and second terms are different, the total transition probability is a sum of each probability. The first term gives a normal constant probability that is computable also by the ordinary S-matrix of plane waves, whereas the second term gives a T -dependent correction that is not computable by the ordinary S-matrix. In ordinary situations, the energy non-conserving terms are negligible but they are important in situations of the present work.

A magnitude of δf and a probability derived from δf depends on a dynamics of the system. When E_{α} and E_{β} are approximate energies of the states $|\alpha\rangle$ and $|\beta\rangle$, we have

$$(E_{\alpha} - E_{\beta}) \langle \beta | S(T) | \alpha \rangle = \langle \beta | O(T) | \alpha \rangle, \quad (33)$$

$$O(T) = i \left\{ \frac{\partial}{\partial T} \Omega_{-}(T) \right\}^{\dagger} \Omega_{+}(T) - i \Omega_{-}^{\dagger} \frac{\partial}{\partial T} \Omega_{+}(T).$$

Hence

$$\delta f = \frac{\langle \beta | O(T) | \alpha \rangle}{E_{\alpha} - E_{\beta}}, \quad (34)$$

and the transition probability to the energy non-conserving states is given in the form,

$$\sum_{\beta} |\delta f|^2 = \sum_{\beta} \left\{ \frac{|\langle \beta | O(T) | \alpha \rangle|^2}{E_{\alpha} - E_{\beta}} \right\} \geq 0, \quad (35)$$

where the equality is satisfied at $T \rightarrow \infty$. States at ultraviolet energy regions couple in a universal manner with the operator $O(T)$ and contribute to the probability at the finite-time interval. Since states of unlimited-momentum couple in Lorentz invariant manner, they give a universal correction to Eq. (32). The finite-size correction appears even in the lowest order of perturbative expansions and is useful for probing the physical system at the large momentum region.

Boundary conditions necessary to determine a solution of a wave equation uniquely in scattering or decay processes are asymptotic boundary conditions [1]. For a scattering from an initial state $|\alpha\rangle$ to a final state $|\beta\rangle$ of a scalar field expressed by $\phi(x)$, the states $|\alpha\rangle$ at $t = -T/2$ are constructed with free waves $\phi_{in}(x)$ and the states $|\beta\rangle$ at $t = T/2$ are constructed with free waves $\phi_{out}(x)$ and satisfy asymptotic boundary conditions,

$$\lim_{t \rightarrow -T/2} \langle \alpha | \phi^f(t) | \beta \rangle = \langle \alpha | \phi_{in}^f | \beta \rangle, \quad (36)$$

$$\lim_{t \rightarrow T/2} \langle \alpha | \phi^f(t) | \beta \rangle = \langle \alpha | \phi_{out}^f | \beta \rangle. \quad (37)$$

The expansion coefficient $\phi^f(t)$ is defined by

$$\phi^f(t) = i \int d^3x f^*(\vec{x}, t) \partial_0 \phi(\vec{x}, t). \quad (38)$$

ϕ_{in}^f and ϕ_{out}^f are defined in the same way. C-number functions $f(\vec{x}, t)$ are normalized and satisfy a free wave equation. The normalized functions decrease fast in space and form a complete set with those functions translated in space. Hence they have central values of position and momentum and the state vector is specified by both variables as $|\vec{p}, \vec{X}\rangle$. Thus matrix elements of $S[T]$ are defined as $\langle \vec{p}_i, \vec{X}_i | S[T] | \vec{p}_j, \vec{X}_j \rangle$ and depend on the position and momentum. The finite-size correction are computed with the position dependence of the probability. For normalized functions to form the complete set, those of different center positions are required [17]. Those of the initial state represent the beam and those of the final state represent a detected particle. They are determined by the experimental apparatus and those of the initial and final states are different normally. Being non-normalizable, plane waves are not suitable for these functions if the damping factor $e^{-\epsilon|t|}$ is not included. Instead, wave packets are normalizable and are suitable. $\phi_{in}(x)$ and $\phi_{out}(x)$ satisfy the free wave equation and the states $|\alpha\rangle$ $|\beta\rangle$ are defined with wave packets. The wave packets which have finite-spatial sizes and decrease fast at large $|\vec{x} - \vec{x}_0|$ ensure the asymptotic conditions at a finite T , where \vec{x}_0 is the center's position. Hence $S[T]$ is described by wave packets and the finite-size corrections are studied with $S[T]$. We present several examples where the finite-size corrections are non-negligible and give interesting observable effects.

3. Quantum particles described by wave packets

Waves of finite sizes expressed by wave packets used for formulating $S[T]$ exist in various areas. Wave functions at the particle zone lose wave nature quickly and time evolution of objects turns to be described by classical equation of motion. Thus a classical mechanical

description is smoothly obtained starting from the quantum mechanical description and physics in this region is understood well by classical physics, as is explained in most textbooks of quantum mechanics. Now in the wave zone, the phase of the wave function remains and gives physical effects that are different from classical physics. They could appear in macroscopic space-time regions. Then their universal properties are common in any wave functions, and can be studied with Gaussian wave packets. Their sizes are determined from physical processes of the particles.

The physics of quantum particles has been neither completely explored nor understood and is becoming relevant to recent advanced science and technology, especially for precision experiments of light particles. Various phenomena of neutrinos and photons caused by these unique phases are studied hereafter. Neutrino interacts extremely weakly with matter and is not disturbed by environment, hence its phase is not washed out, consequently the neutrino retains the wave nature even in macroscopic area and reveals large finite-size corrections [18, 19]. The finite-size correction is observed as a diffraction pattern of the neutrino produced in a decay of the pion and in other processes that the neutrino gives rise to.

Photon is massless in vacuum and behaves approximately like a particle of small mass in high-energy region in dilute matter. Normally, the quantum mechanical phase of single low-energy photon is washed out and a large number of these photons behave like a classical electromagnetic wave in macroscopic areas. In various exceptional situations, its phase is not washed out and photons reveal unusual properties and interact with microscopic objects as single quanta. The photon then is expressed by a wave packet and the probability to detect it at a finite distance shows the diffraction behavior of a single quantum. They lead also the photons to have unusual thermodynamic property.

Waves of small sizes move like classical particles [20–30] and exhibit wave-like behaviors such as anomalous finite-size corrections in scattering cross sections or decay rates, and are called quantum particles in the present paper. Quantum particles of relativistic waves have universal properties.

3.1. Symmetric wave packets

The Gaussian wave packet of a relativistic particle of mass m and the central momentum \vec{p}_0 , position \vec{X}_0 , and time T_0 is expressed in the momentum representation by

$$\langle t, \vec{p} | \vec{p}_0, \vec{X}_0, T_0 \rangle = N \sigma^{3/2} e^{-iE(\vec{p})(t-T_0) - i\vec{p} \cdot \vec{X}_0 - \frac{\sigma}{2} (\vec{p} - \vec{p}_0)^2}, \quad (39)$$

where σ is a spatial size of the wave packet, N is normalization factor and the energy is given by a relativistic form, $E(\vec{p}) = \sqrt{\vec{p}^2 + m^2}$. This is a superposition of eigenstates of the energy and momentum of the widths $\frac{|\vec{p}|}{E(\vec{p})\sqrt{\sigma}}$ and $\frac{1}{\sqrt{\sigma}}$ respectively, and is a simple Gaussian form of \vec{p} at $t = T_0$, and retains its shape afterward. The completeness of wave packets of the continuous center position and momentum and other important properties were given in Ref. [17]. Some of them are summarized in the following for a completeness of the present paper. They satisfy

$$\int d\vec{X} \frac{d\vec{p}}{(2\pi)^3} |\vec{p}, \vec{X}, T\rangle \langle \vec{p}, \vec{X}, T| = 1, \quad (40)$$

and the wave function in coordinate representation is

$$w(\vec{p}_0, x) = \langle t, \vec{x} | \vec{p}_0, \vec{X}_0, T_0 \rangle = \int d\vec{k} \langle \vec{x} | \vec{k} \rangle \langle t, \vec{k} | \vec{p}_0, \vec{X}_0, T_0 \rangle, \quad (41)$$

and becomes also a Gaussian form in \vec{x} around a new center

$$w(\vec{p}_0, x) = N e^{-\frac{1}{2\sigma}(\vec{x}-\vec{X}_0-\vec{v}_0(t-T_0))^2} e^{-iE(\vec{p}_0)(t-T_0)+i\vec{p}_0\cdot(\vec{x}-\vec{X}_0)}, \quad (42)$$

$$\vec{v}_0 = \frac{\partial}{\partial p_i} E(\vec{p})|_{\vec{p}=\vec{p}_0},$$

in a small $|t - T_0|$ region. Thus the wave function keeps the shape and moves with a velocity \vec{v}_0 and the modulus is invariant under

$$t \rightarrow t + \delta t, \quad \vec{x} \rightarrow \vec{x} + \vec{v}_0 \delta t. \quad (43)$$

Since the position of the wave packet moves uniformly with the velocity \vec{v}_0 and has the extension σ , the wave function becomes finite only inside a narrow strip of this width. Hence the quantum state expressed by this wave packet behaves like a particle of the extension σ . At a large $|t - T_0|$, the function expands.

The wave functions Eq. (42) decrease rapidly with $|\vec{x} - \vec{X}_0 - \vec{v}_0(t - T_0)|$ and vanish at $|\vec{x} - \vec{X}_0 - \vec{v}_0(t - T_0)| \rightarrow \infty$. Hence they satisfy the asymptotic boundary conditions and are appropriate to use as basis, $f(\vec{x}, t)$, of Eq. (38). The transition process of the particle prepared at the initial time T_i and of observing the final states at a final time T_f of a finite $T = T_f - T_i$, is studied with the S-matrix at the finite-time interval $S[T]$ thus defined. Because the S-matrix of plane waves defined at $T = \infty$, $S[\infty]$, satisfy the boundary condition at $t = \pm\infty$, that is different from $S[T]$ defined at $t = \pm T/2$. $S[T]$ defined by the wave packets Eq. (42), and the amplitudes and probabilities obtained from them are not equivalent to those obtained from $S[\infty]$ generally in the wave zone. Then, the computations should be made with $S[T]$. Conversely if they are equivalent, the computations can be made with either methods.

The kinetic energy is strictly conserved in both classical collisions of particles under a force of finite range and quantum collisions described by $S[\infty]$ of the stationary states of the free Hamiltonian, whereas the conservation law of the kinetic energy is slightly modified in a collision of the finite-time interval T described by $S[T]$ from the algebra Eq. (31). The total energy is conserved, but is different from the kinetic energy in the space-time region where the interaction Hamiltonian has a finite expectation value. Hence the kinetic energy is not conserved in this region. The non-conservation of the kinetic energy is a unique property of quantum particles described by $S[T]$ and causes unusual behaviors to the collision or decay probabilities.

The quantum states of finite-spatial extensions are expressed by superpositions of plane waves of different momenta and energies, and their scatterings are those of the non-stationary states. These non-stationary wave packets are specified by the values of position, momentum, and complex phase at the center. Even though its spatial size is so small that it behaves like a point particle, a wave nature represented by the phase remains. The phase that depends on dynamical variables gives physical effects that are characteristic of the quantum particles.

σ in Gaussian wave packet determines the spatial size of quantum particle, and depends on the situations. Because the probability to detect this particle is unity inside the wave packet, this size is a classical size of a quantum particle. So, σ for out-going state is the size of the unit of detecting system that gives a signal, and is a size of nucleus used in detector for the neutrino. For a high-energy photon, the signal is taken from its e^+e^- creation around an electric field of the nucleus used in detector, hence σ is about the size of nucleus. σ for

in-state is also the size of wave function that expresses this particle. This size is infinite for the idealistic particle in vacuum, but is finite in matter due to effects of environment. When a particle expressed by a certain wave function interacts with others and the both make a transition to other states, this particle is expressed by one wave function in a finite time-interval between these reactions. Hence that is determined by a mean free time of this particle. Thus σ is determined by the mean free path for in-coming waves. σ for pion, kaon, muon, proton, photon, and electron in the initial states are estimated from their mean free paths in the matter of experiments. Actually most of them are macroscopic sizes in high-energy regions. An electron easily loses energy by electromagnetic showers and is exceptional. In low-energy regions, an electron, negative muon, and negative pion form bound states of microscopic sizes with nucleus in matter, and σ are microscopic sizes. Positive charged particles such as positive muon and positive pion do not form the bound states with nucleus and may have larger σ .

Thus σ of a nuclear size, atomic size, or larger size appear depending on the situation. In a scattering or decay of waves with different sizes, the wave functions overlap in finite and asymmetric region. Consequently conservation laws derived from space-time symmetry are modified.

3.2. Local interaction

Characteristic features of quantum particles are connected with the phase factor of wave functions and appear in the lowest order of interactions of scalar fields. Hence we study scattering of particles caused by the local interaction

$$\mathcal{L}_{int} = g \prod_{j=1}^{j=N} \varphi_j(x), \quad (44)$$

in the lowest order of g first. Effects of spin and internal structure will be included later. Interactions of N_1 in-coming and N_2 out-going particles expressed by the wave packets parameterized by $(\vec{p}_i, \vec{X}_i, T_i; \sigma_i)$ at a space-time position (t, \vec{x}) is given in the form [17],

$$\begin{aligned} \langle j | \prod_{j=1}^{j=N} \varphi_j(x) | l \rangle &= \prod_{k=1}^{N_1} w_k^*(x, \vec{p}_k; X_k, T_k, \sigma_k) \times \prod_{l=1}^{N_2} w_l(x, \vec{p}_l; X_l, T_l, \sigma_l) \\ &= N_t e^{-\frac{1}{2\sigma_s}(\vec{x}-\vec{x}_0(t))^2 - \frac{1}{2\sigma_t}(t-t_0)^2} e^{R+i\phi}, \\ N_t &= \prod_{k,l} N_k^* N_l, \end{aligned} \quad (45)$$

where σ_s and σ_t in the exponent display the extents in \vec{x} and t and are expressed in the form:

$$\frac{1}{\sigma_s} = \sum_j \frac{1}{\sigma_j}, \quad \frac{1}{\sigma_t} = \sum_j \frac{\vec{v}_j^2}{\sigma_j} - \frac{\vec{v}_0^2}{\sigma_s}, \quad (46)$$

$$\vec{v}_0 = \sigma_s \sum_j \frac{\vec{v}_j}{\sigma_j}, \quad \vec{v}_j = \frac{\vec{p}_j}{E_j}. \quad (47)$$

Here, $\vec{x}_0(t)$ is the center in \vec{x} and moves with \vec{v}_0 ,

$$\begin{aligned}\vec{x}_0(t) &= \vec{v}_0 t + \vec{x}_0(0), \\ \vec{x}_0(0) &= \sigma_s \left\{ \sum_j \frac{\tilde{\vec{X}}_j}{\sigma_j} - i \sum_j (\pm) \vec{p}_j \right\}, \\ t_0 &= \sigma_t \left\{ \frac{\vec{v}_0 \cdot \vec{x}_0}{\sigma_s} - \sum_j \frac{\vec{v}_j \cdot \tilde{\vec{X}}_j}{\sigma_j} + i \sum_j (\pm) E(\vec{p}_j) \right\}, \\ \tilde{\vec{X}}_j &= \vec{X}_j - \vec{v}_j T_j.\end{aligned}\tag{48}$$

In above equations and hereafter, (+) and (−) are for in-coming and out-going states, respectively. The real part of the exponent of Eq. (45), R , determines the magnitude and is composed of the position-dependent and momentum-dependent terms. The former, $R_{trajectory}$, and the latter, $R_{momentum}$, are expressed by,

$$R = R_{trajectory} + R_{momentum},\tag{49}$$

$$R_{trajectory} = - \sum_j \frac{\tilde{\vec{X}}_j^2}{2\sigma_j} + 2\sigma_s \left(\sum_j \frac{\tilde{\vec{X}}_j}{2\sigma_j} \right)^2 + 2\sigma_t \left(\sum_j \frac{(\vec{v}_0 - \vec{v}_j) \cdot \tilde{\vec{X}}_j}{2\sigma_j} \right)^2,\tag{50}$$

$$R_{momentum} = - \frac{\sigma_t}{2} \left\{ \sum_j (\pm) (E(\vec{p}_j) - \vec{v}_0 \cdot \vec{p}_j) \right\}^2 - \frac{\sigma_s}{2} \left(\sum_j (\pm) \vec{p}_j \right)^2.\tag{51}$$

From $R_{trajectory}$, the particles follow classical orbits and from $R_{momentum}$, Eq. (51), they follow the approximate energy-momentum conservation. Because the interacting system is invariant under a translation of the coordinate system, $R_{trajectory}$ is invariant under the translation

$$\vec{X}_i \rightarrow \vec{X}_i + \vec{d}, \quad T_i \rightarrow T_i + \delta,\tag{52}$$

where (δ, \vec{d}) is a constant four vector. From $R_{momentum}$, the momentum is approximately conserved with the uncertainty $1/\sqrt{\sigma_s}$ and the energy of the system moving with \vec{v}_0 is approximately conserved with the uncertainty $1/\sqrt{\sigma_t}$. Since a massless particle has the maximum speed, the moving frame has a large velocity and the effect becomes significant for the massless or extremely light particle. The product Eq. (45) depends also on the phase factor

$$\begin{aligned}\phi &= \phi_0 + \phi_1, \\ \phi_0 &= \sum_j (\pm) (\vec{p}_j \cdot \vec{X}_j - E(\vec{p}_j) T_j), \\ \phi_1 &= -2\sigma_t \left(\sum_j \frac{(\vec{v}_0 - \vec{v}_j) \cdot \tilde{\vec{X}}_j}{2\sigma_j} \right) \left\{ \sum_j (\pm) (\vec{v}_0 \cdot \vec{p}_j - E(\vec{p}_j)) \right\} \\ &\quad - 2\sigma_s \left(\sum_j (\pm) \vec{p}_j \right) \cdot \left(\sum_j \frac{\tilde{\vec{X}}_j}{2\sigma_j} \right),\end{aligned}\tag{53}$$

where ϕ_0 agrees with that of a plane wave.

When the values of σ_s and σ_t are finite, the product Eq.(45) becomes finite in a small region of (t, \vec{x}) and decreases steeply away from this region. Hence the integration over (t, \vec{x}) becomes

$$\int d^4x \langle j | \prod_{j=1}^{j=N} \varphi_j(x) | l \rangle = N_t (2\sigma_s \pi)^{\frac{3}{2}} (2\sigma_t)^{\frac{1}{2}} e^{R+i\phi}, \quad (54)$$

and converges fast. The integral over $0 \leq t \leq T$ becomes $O(e^{-\frac{T^2}{2\sigma_t}})$. Thus the finite-size correction to the probability is $O(e^{-\frac{T^2}{2\sigma_t}})$ with a microscopic σ_t , and is negligible at a macroscopic T .

3.3. Pseudo-Doppler effect

First effect caused by the modified conservation law of kinetic energy is the distortion of the energy distribution, which appears in the amplitude at a finite and infinite T .

The energy-momentum conservation in an invariant system under the translation

$$x_\mu \rightarrow x_\mu + d_\mu, \quad (55)$$

where d_μ is a constant four vector, is derived from the integration for the plane waves

$$\int d^4x e^{i(k_i - k_f) \cdot x} = (2\pi)^4 \delta^{(4)}(k_i - k_f), \quad (56)$$

where k_i and k_f are the four-dimensional momenta of the initial and final states. In the amplitude of the wave packets, the wave functions overlap in a finite space-time area and the amplitude is not invariant under Eq.(55), but is approximately invariant for a small σ_t under the transformation Eq.(43). Hence the energy in the moving frame Eq.(51), is approximately conserved. In a system of $\sigma_t = \infty$, the invariance is rigorous.

R_{momentum} is rewritten as

$$\begin{aligned} R_{\text{momentum}} &= -\frac{\sigma_t}{2} (\delta \tilde{E})^2 - \frac{\sigma_s}{2} (\delta \vec{p})^2, \\ \delta \tilde{E} &= \sum_{\text{initial}, j} (E^i(\vec{p}_j) - \vec{v}_0 \cdot \vec{p}_j^i) - \sum_{\text{final}, k} (E^f(\vec{p}_k) - \vec{v}_0 \cdot \vec{p}_k^f), \\ \delta \vec{p} &= \sum_j (\pm) \vec{p}_j. \end{aligned} \quad (57)$$

For small σ_s and large σ_t , $|\delta \vec{p}|$ becomes large but $|\delta \tilde{E}|$ becomes small, and the modified conservation law, $\delta \tilde{E} = 0$,

$$\sum_{\text{final}} E^i(\vec{p}_j) - \sum_{\text{initial}} E^f(\vec{p}_k) = \sum_{\text{final}} \vec{v}_0 \cdot \vec{p}_j^i - \sum_{\text{initial}} \vec{v}_0 \cdot \vec{p}_k^f, \quad (58)$$

is fulfilled. The momentum spreading is large and the conservation law for the events of $\delta \vec{p} = 0$ or $\vec{v}_0 = 0$ becomes the form:

$$\sum_{\text{final}} E^i(\vec{p}_j) - \sum_{\text{initial}} E^f(\vec{p}_k) = 0. \quad (59)$$

For the events of $\delta \vec{p} \neq 0$ and $\vec{v}_0 \neq 0$, the law becomes

$$\sum_{\text{final}} \gamma_j E^i(\vec{p}_j) - \sum_{\text{initial}} \gamma_k E^f(\vec{p}_k) = 0, \quad \gamma_j = \frac{E^i(\vec{p}_j) - \vec{v}_0 \cdot \vec{p}_j^i}{E^j(\vec{p}_j)}, \quad (60)$$

where γ_j is the rate of the energies in the moving and rest systems. $\delta\tilde{E}$ is also written in high-energy region in the following form:

$$\delta\tilde{E} = \sum_j (\pm) E(\tilde{\vec{p}}_j), \quad \tilde{\vec{p}}_j = \vec{p}_j - \frac{\sigma_s}{\sigma_j} \delta\vec{p}. \quad (61)$$

From the momenta and energies of particles in the final state, $\tilde{\vec{p}}_j$ can be computed from Eq. (61), and $E(\tilde{\vec{p}}_j)$ is calculated. Then Eq. (58) can be verified. The total momenta are distributed with the width given by $1/\sqrt{\sigma_s}$ but the sum of total energies at $\tilde{\vec{p}}_j$ vanishes at each event. Even though the detector is at rest and a real Doppler effect is irrelevant, the kinetic energy of the moving frame, instead of that in the rest system, is conserved. Consequently the kinetic energy of the final state shifts in magnitude in events of large $|\delta\vec{p}|$. In Doppler effect, the energy shifts in all events, so the shifts due to the wave packet is different and called pseudo-Doppler effect.

For small σ_s and σ_t , $|\delta\vec{p}|$ and $|\delta E(\tilde{\vec{p}}_j)|$ become large. For plane waves, $\sigma_i = \infty$, the velocity \vec{v}_0 vanishes and the modified conservation law becomes the standard one. Thus the energy-conservation for the wave packets is different from both of the classical mechanics and of the plane waves of the quantum mechanics.

The modified law of energy conservation results from $S[\infty]$ that satisfies the commutation relation $[S[\infty], H_0] = 0$ due to the fact that the wave packets are superpositions of states of continuous eigenvalues of H_0 . The quantum particle of the momentum and kinetic energy, \vec{p} and $E(\vec{p})$, and size σ makes a reaction as a particle of the energy $\gamma E(\vec{p})$ and the modified conservation law, Eq. (60), is fulfilled. Here γ_i is regarded as a ratio of the time intervals in the moving and rest frames and Eq. (58), is understood as that for the average values taken over the time intervals

$$\frac{1}{\sum_j \gamma_j} \left\{ \sum_j \gamma_j E(\vec{p}_j) - \sum_k \gamma_k E(\vec{p}_k) \right\} = \langle E^i \rangle - \langle E^f \rangle = 0. \quad (62)$$

Thus the conservation law of energy is modified to that for the average values. Because the energy is conjugate to the time, the equality of average values taken over the time intervals is reasonable. From Eq. (58), the effective action

$$\int \sum_i (E_i dt - \vec{p}_i \cdot d\vec{x}_i) = \int \sum_i (E_i - \vec{p}_i \cdot \vec{v}_i) dt, \quad \vec{v}_i = \vec{v}_0, \quad (63)$$

of the initial state coincides with that of the final state in the present reaction.

3.4. Finite-size correction

Second effect caused by the modified conservation law is the large finite-size correction. If σ_t is finite of a microscopic size, the integration over t converges and the amplitude and probability decrease rapidly due to $R_{trajectory}$. In a marginal case of $\sigma_t = \infty$, modulus of Eq. (45) does not decrease with t but wave packets overlap in the infinite-time interval. This happens in various situations. If all the particles except a particle 1 are plane waves,

$$\sigma_1 \neq \infty, \quad (64)$$

$$\sigma_i = \infty, \quad i \neq 1, \quad (65)$$

the frequency and the real and imaginary parts of the amplitude

$$\prod_j N_j^* \prod_l N_l e^{-\frac{1}{2\sigma_s}(\vec{x}-\vec{x}_0(t))^2 - i\omega(t-t_0)} e^{R+i\phi}, \quad (66)$$

$$\sigma_s = \sigma_1, \quad \sigma_t = \infty,$$

are

$$\omega = \sum_{initial} E_i - \sum_{final} E_j - \vec{v}_1 \cdot \delta\vec{p}, \quad (67)$$

$$R = R_{momentum} + R_{trajectory},$$

$$R_{momentum} = -\frac{\sigma_1}{2}(\delta\vec{p})^2, \quad R_{trajectory} = 0,$$

$$\phi = E(\vec{p}_1)T_1 - \vec{p}_1 \cdot \vec{X}_1 - \delta\vec{p} \cdot \vec{X}_1.$$

The modulus of Eq. (66) decreases fast with $|\vec{x} - \vec{x}_0(t)|$ and the total momentum is approximately conserved, whereas that is constant in t . The phase factor has a similar form to that of the plane wave Eq. (42) but the angular velocity ω is not identical. ω in Eq. (67) is an energy in a moving frame of the velocity \vec{v}_1 of showing the pseudo-Doppler effect, and is

$$\omega = -E_1(\vec{p}_1) + \vec{v}_1 \cdot \vec{p}_1 + \omega_0 = -(\sqrt{\vec{p}_1^2 + m_1^2} - |\vec{p}_1|) + \omega_0$$

$$= -\frac{m_1^2}{2|\vec{p}_1|} + \omega_0, \quad (68)$$

where m_1 is the mass of 1 and ω_0 is independent of \vec{p}_1 at high-energy region. Hence ω depends on the momentum of particle 1 differently from the plane wave, and there are more states satisfying $\omega \approx 0$ than those of the simple plane wave. The amplitude Eq. (66) at a large-time interval is determined by a state of satisfying $\omega = 0$ and also the states of $\omega \approx 0$. From Eq. (68), ω is degenerate at $|\vec{p}_1| \rightarrow \infty$, and infinite number of states give the contribution. It will be shown that the rate derived from this at a finite T , $\Gamma(T)$, has the large finite-size correction and is described in the form,

$$\Gamma(T) = \Gamma_0 + \Gamma_1(T), \quad (69)$$

$$\Gamma_1(T) = C_1/T,$$

where C_1 is a constant and Γ_0 is the asymptotic term.

σ_t becomes infinite when the right-hand side of Eq. (46) vanishes. This condition is fulfilled in particular momenta of the initial and final states. The probability has the finite-size correction in this kinematical region, then.

3.5. Asymmetric wave packet

In some situations, the wave packet is asymmetric in \vec{k}_L and \vec{k}_T which are parallel and perpendicular to the central momentum, or in \vec{k} and $|\vec{k}|$. The small energy uncertainty, $\delta E \ll |\vec{k}|$ also often appears. For an asymmetric wave packet or a wave packet with different spreadings in the momentum and energy, we have

$$\langle t, \vec{p} | \vec{p}_0, \vec{X}_0, T_0 \rangle_{asy} = N \sigma^{\frac{3}{2}} e^{-iE(\vec{p})(t-T_0) - i\vec{p} \cdot \vec{X}_0 - \frac{\sigma_L}{2}(\vec{p}_L - \vec{p}_L^0)^2 - \frac{\sigma_T}{2}(\vec{p}_T)^2}, \quad (70)$$

$$\langle t, \vec{p} | \vec{p}_0, \vec{X}_0, T_0 \rangle_E = N \sigma^{\frac{3}{2}} e^{-iE(\vec{p})(t-T_0) - i\vec{p} \cdot \vec{X}_0 - \frac{\sigma}{2}(\vec{p} - \vec{p}_0)^2 - \frac{\sigma_E}{2}(E(\vec{p}) - E_0)^2}, \quad (71)$$

where σ_L , σ_T , and σ_E are a size in the parallel and perpendicular directions to the center of momentum, and that in the energy. The functions in coordinate representation become

Gaussian forms in \vec{x} and t .

$$\begin{aligned}\langle t, \vec{x} | \vec{p}_0, \vec{X}_0, T_0 \rangle_{asy} &= \int d\vec{p} \langle \vec{x} | \vec{p} \rangle \langle t, \vec{p} | \vec{p}_0, \vec{X}_0, T_0 \rangle_{asy} \\ &= N \sigma^{\frac{3}{2}} e^{-iE(\vec{p}_0)(t-T_0) - i\vec{p}_0 \cdot \vec{X}_0 - \frac{1}{2\sigma_L}(x_L - X_L - v(t-T_0))^2 - \frac{1}{2\sigma_T}(\vec{x}_T)^2},\end{aligned}\quad (72)$$

$$\langle t, \vec{x} | \vec{p}_0, \vec{X}_0, T_0 \rangle_E = \int d\vec{p} \langle \vec{x} | \vec{p} \rangle \langle t, \vec{p} | \vec{p}_0, \vec{X}_0, T_0 \rangle_E. \quad (73)$$

In $\sigma_L \approx \sigma_T$ or $\sigma_E \approx \sigma$, the energy spreading is about the same as that of the momentum, and the probability for a finite $|\Delta\vec{p}|$ around the central momentum \vec{p}_0 has the pseudo-Doppler and finite-size effects. In $\sigma_L \gg \sigma_T$ or $\sigma_E \gg \sigma$, on the other hand, the energy spreading is much smaller than the momentum spreading and **Eq.** (72) or (73) is applied. Precision experiments of $\Delta E \approx 0, |\Delta\vec{p}| = \infty$ of narrow energy levels are studied with the expression (73), and the probability does not have pseudo-Doppler and finite-size effects then.

4. Two-body decay: $A \rightarrow B + C$

Unusual properties of the decay probability at a finite distance are studied in detail for two-body decay here. Decay rate is computed with $S[T]$ and the finite-size correction to that computed by Fermi's golden rule is found. The correction depends on the boundary conditions of the experiments and is computed properly with $S[T]$ that satisfies the boundary condition at T , instead of $S[\infty]$.

Two-body decays of a particle A into B and C of masses m_A , m_B and m_C satisfying $m_A > m_B + m_C$ and governed by a local Lagrangian

$$\begin{aligned}\mathcal{L} &= \mathcal{L}_0 + \mathcal{L}_{int}, \\ \mathcal{L}_0 &= \frac{1}{2}[(\partial\varphi_A)^2 - m_A^2\varphi_A^2 + (\partial\varphi_B)^2 - m_B^2\varphi_B^2 + (\partial\varphi_C)^2 - m_C^2\varphi_C^2], \\ \mathcal{L}_{int} &= g\varphi_A(x)\varphi_B(x)\varphi_C(x),\end{aligned}\quad (74)$$

in the wave zone are studied in the lowest order of coupling constant g . The characteristic features of decay amplitude in the wave packet scattering is seen from Fig. (2) that shows a space-time picture of the decay of A of a large size to a large B and C of a small size. Because the interaction occurs in the finite region where these waves overlap, the conservation laws of the kinetic energy and momentum are modified from those of plane waves.

4.1. Average energy in the wave zone

A kinetic energy of the wave function at a finite t is not a constant. A state vector evolves with the Schrödinger equation of a total Hamiltonian composed of the free part H_0 and the interaction part H_{int} derived by the Lagrangian, Eq. (74)

$$i\hbar \frac{\partial}{\partial t} |\Psi(t)\rangle = (H_0 + H_{int}) |\Psi(t)\rangle. \quad (75)$$

From perturbative expansion, a solution satisfying the boundary condition $|\Psi(0)\rangle = |\psi_1\rangle$ is,

$$|\Psi(t)\rangle = a_1(t)|\psi_1\rangle + |\psi_2\rangle, \quad (76)$$

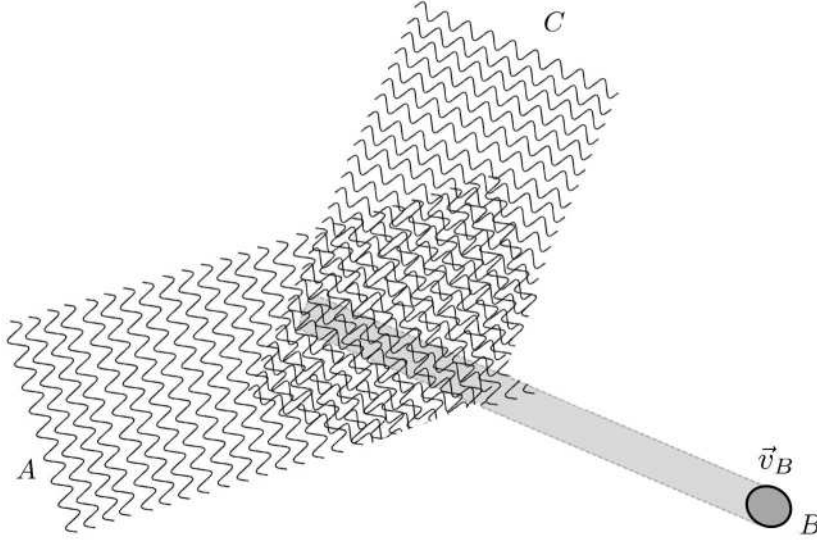


Fig. 2 The decay amplitude of A to B and C which are expressed with wave packets of different sizes are represented. They interact in a region where they overlap. If the size of B is smaller than others, the region is mainly determined by B .

where $|\psi_1\rangle$ is one-particle state composed of A of a momentum \vec{p}_A and a kinetic energy E_A and $|\psi_2\rangle$ is a two-particle state composed of B and C

$$|\psi_1(t)\rangle = e^{\frac{E_A}{i\hbar}t} |A, \vec{p}_A\rangle, \quad (77)$$

$$|\psi_2(t)\rangle = \int_0^t dt' \frac{H_{int}(t')}{i\hbar} |\psi_1(t')\rangle = \int_0^t dt' |B, C\rangle \langle B, C| \frac{H_{int}(t')}{i\hbar} |\psi_1(t')\rangle. \quad (78)$$

In the lowest order in g ,

$$a_1(t) = 1. \quad (79)$$

An energy expectation value is

$$\langle E \rangle = \frac{\langle \Psi(t) | H | \Psi(t) \rangle}{\langle \Psi(t) | \Psi(t) \rangle}, \quad (80)$$

$$\begin{aligned} \langle \Psi(t) | H | \Psi(t) \rangle &= |a_1(t)|^2 E_A \langle \psi_1 | \psi_1 \rangle + 2 \text{Re} [a_1(t) \langle \psi_2 | H_{int} | \psi_1 \rangle] + (E_B + E_C) \langle \psi_2 | \psi_2 \rangle, \\ \langle \Psi(t) | \Psi(t) \rangle &= |a_1(t)|^2 \langle \psi_1 | \psi_1 \rangle + \langle \psi_2 | \psi_2 \rangle. \end{aligned}$$

At the infinite t ,

$$\langle \psi_2 | \psi_2 \rangle = (2\pi)t\delta(\omega) \left| \langle B, C | \frac{H_{int}(0)}{i\hbar} | A \rangle \right|^2, \quad (81)$$

$$a_1(t) \langle \psi_2 | H_{int} | \psi_1 \rangle = \frac{i}{\omega} (1 - e^{-i\omega t/\hbar}) \left| \langle B, C | \frac{H_{int}(0)}{i\hbar} | A \rangle \right|^2 = O(1), \quad (82)$$

$$\omega = E_A - E_B - E_C,$$

hence the expectation value of the interaction $H_{int}(0)$, Eq.(82), is negligible compared to Eq.(81) and the kinetic energy as well as the total energy is E_A . Now for the finite t , the

expectation value of $H_{int}(0)$ is not negligible. An average over a finite-time interval gives

$$2Aver(Re[a_1(t)\langle\psi_2|H_{int}|\psi_1\rangle]) = \frac{2}{\omega} \left| \langle B, C | \frac{H_{int}(0)}{i\hbar} | A \rangle \right|^2, \quad (83)$$

$$Aver(\langle\psi_2|\psi_2\rangle) = 2\frac{\hbar^2}{\omega^2} \left| \langle B, C | \frac{H_{int}(0)}{i\hbar} | A \rangle \right|^2, \quad (84)$$

$$Aver(\langle\psi_2|H_0|\psi_2\rangle) = 2(E_B + E_C)\frac{\hbar^2}{\omega^2} \left| \langle B, C | \frac{H_{int}(0)}{i\hbar} | A \rangle \right|^2. \quad (85)$$

The expectation value of the total energy becomes

$$Aver\langle H \rangle = E_A. \quad (86)$$

Thus the average energy coincides with the initial energy, but the average kinetic energy is

$$Aver(\langle H_0 \rangle) = \frac{E_A + 2(E_B + E_C)\frac{2\hbar^2}{\omega^2} |\langle B, C | \frac{H_{int}(0)}{i\hbar} | A \rangle|^2}{1 + \frac{2\hbar^2}{\omega^2} |\langle B, C | \frac{H_{int}(0)}{i\hbar} | A \rangle|^2}, \quad (87)$$

and is different from the initial kinetic energy. H_{int} causes a transition of A to B and C , and is non-diagonal in the base of eigenvectors defined by H_0 . Thus H_{int} does not contribute to the total energy in the infinite t , but at a finite t , the state $|\Psi(t)\rangle$ is a superposition of $|A\rangle$ and $|B, C\rangle$ and H_{int} has a finite expectation value. The total energy is always the same but the expectation value of H_{int} is finite in a finite t . Hence the state becomes a superposition of different kinetic energies and the kinetic energy is not a good quantum number in this region.

E_A is real in the lowest order of g and has an imaginary part in the second order, which represents a life time of A , τ_A . In $t \ll \tau_A$, the imaginary part of E_A is negligible. For a self-consistent treatment of the decay process, we start from E_A of an imaginary part and compute the decay amplitude and probability. The decay probability is proportional to T in $T \ll \tau_A$ and becomes unity at $T \gg \tau_A$.

4.2. Transition amplitude and decay probability

Next we study the transition probability at a finite distance. A decay of a particle A at a space-time position (\vec{X}_A, T_A) into particles B at (\vec{X}_B, T_B) and C at (\vec{X}_C, T_C) in the most general case of the symmetric wave packets

$$\sigma_A, \sigma_B, \sigma_C, \quad (88)$$

of the four-dimensional momenta and masses

$$(E_A, \vec{p}_A; m_A), (E_B, \vec{p}_B; m_B), (E_C, \vec{p}_C; m_C), \quad (89)$$

is studied here. A life time of A expressed with an imaginary part of E_A is assumed negligible in majority places of the present paper. From the interaction Lagrangian Eq. (74), the transition amplitude is expressed with an integral over (t, \vec{x})

$$\begin{aligned} \mathcal{M}(A \rightarrow B + C) &= g \int dt \int d\vec{x} e^{-\frac{1}{2\sigma_s}(\vec{x}-\vec{x}_0)^2 - \frac{1}{2\sigma_t}(t-t_0)^2} e^{R+i\phi} \\ &= g(2\pi\sigma_s)^{\frac{3}{2}}(2\pi\sigma_t)^{\frac{1}{2}} e^{R+i\phi} \theta(\vec{X}_i, T_i), \end{aligned} \quad (90)$$

for finite values of σ_s and σ_t , where $\theta(\vec{X}_i, T_i)$ denotes the conditions that t_0 is the inside of the time region defined from the boundary conditions and we omit to write it hereafter. σ_s

and σ_t are given in the expressions

$$\frac{1}{\sigma_s} = \frac{1}{\sigma_A} + \frac{1}{\sigma_B} + \frac{1}{\sigma_C}, \quad (91)$$

$$\frac{1}{\sigma_t} = \frac{v_A^2}{\sigma_A} + \frac{v_B^2}{\sigma_B} + \frac{v_C^2}{\sigma_C} - \sigma_s \left(\frac{\vec{v}_A}{\sigma_A} + \frac{\vec{v}_B}{\sigma_B} + \frac{\vec{v}_C}{\sigma_C} \right)^2. \quad (92)$$

The center position $\vec{x}_0(t)$ is

$$\vec{x}_0(t) = \vec{x}_0(0) + \vec{v}_0(t - t_0), \quad (93)$$

of an average velocity \vec{v}_0 ,

$$\vec{v}_0 = \sigma_s \left(\frac{\vec{v}_A}{\sigma_A} + \frac{\vec{v}_B}{\sigma_B} + \frac{\vec{v}_C}{\sigma_C} \right). \quad (94)$$

R and ϕ in the exponent are obtained from Eqs. (50), (51), and (53) and are given as,

$$R = R_{\text{trajectory}} + R_{\text{momentum}}, \quad (95)$$

$$R_{\text{trajectory}} = - \sum_j \frac{\tilde{X}_j^2}{2\sigma_j} + 2\sigma_s \left(\sum_j \frac{\tilde{X}_j}{2\sigma_j} \right)^2 + 2\sigma_t \left(\sum_j \frac{(\vec{v}_0 - \vec{v}_j) \cdot \tilde{X}_j}{2\sigma_j} \right)^2, \quad (96)$$

$$R_{\text{momentum}} = -\frac{\sigma_t}{2}(\delta E - \vec{v}_0 \cdot \delta \vec{p})^2 - \frac{\sigma_s}{2}(\delta \vec{p})^2, \quad (97)$$

$$\delta E = E_A(\vec{p}_A) - E_B(\vec{p}_B) - E_C(\vec{p}_C), \quad \delta \vec{p} = \vec{p}_A - \vec{p}_B - \vec{p}_C,$$

and ϕ is a function of the momenta \vec{p}_j and positions \vec{X}_j .

Since $R_{\text{trajectory}}$ is a function of the momenta and coordinates, we write it as $R_{\text{trajectory}}(\vec{X}_A, T_A; \vec{X}_l, T_l)$, where l stands for B or C . This is invariant under the translation, Eq. (52)

$$R_{\text{trajectory}}(\vec{X}_A + \vec{d}, T_A + \delta; \vec{X}_l + \vec{d}, T_l + \delta) = R_{\text{trajectory}}(\vec{X}_A, T_A; \vec{X}_l, T_l), \quad (98)$$

and is a function of the variables $\tilde{X}_l = \vec{X}_l - \vec{v}_l T_l$. Hence the left-hand side of the above equation is written as,

$$R_{\text{trajectory}}(\vec{X}_A + \vec{d} - \vec{v}_A \delta, T_A; \vec{X}_l + \vec{d} - \vec{v}_l \delta, T_l). \quad (99)$$

Choosing $\vec{d} = \vec{v}_A \delta$, we have the identity:

$$R_{\text{trajectory}}(\vec{X}_A, T_A; \vec{X}_l + \vec{v}_A \delta - \vec{v}_l \delta, T_l) = R_{\text{trajectory}}(\vec{X}_A, T_A; \vec{X}_l, T_l), \quad (100)$$

and

$$\frac{\partial}{\partial \delta} R_{\text{trajectory}}(\vec{X}_A, T_A; \vec{X}_l + \vec{v}_A \delta - \vec{v}_l \delta, T_l) = 0. \quad (101)$$

The probability is the integral

$$P = \int \prod_i d\vec{X}_i \frac{d\vec{p}_i}{(2\pi)^3} |\mathcal{M}|^2. \quad (102)$$

$|\mathcal{M}|^2$ does not depend on δ from Eq. (101), and the phase space is reduced to that in δ component and the orthogonal components, \vec{X}_T ,

$$\int d\delta \prod_i d\vec{X}_{T,i} \frac{d\vec{p}_i}{(2\pi)^3} |\mathcal{M}|^2. \quad (103)$$

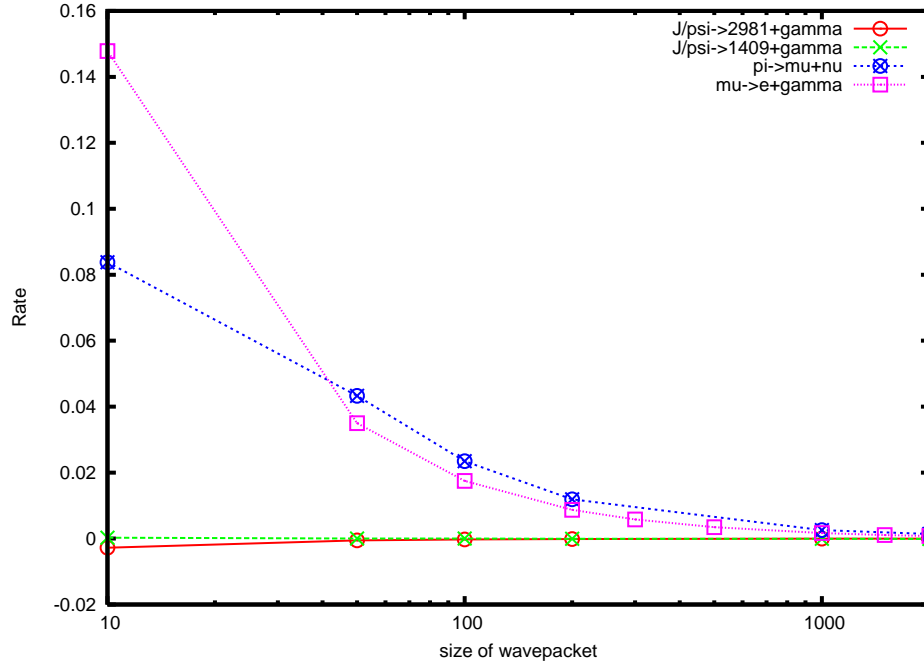


Fig. 3 The probabilities of decays at rest Eq. (104) for the wave packet in two-body decays, $J/\Psi \rightarrow M(2981) + \gamma$ (red solid), $J/\Psi \rightarrow \eta(1409) + \gamma$ (green dot), $\pi \rightarrow \mu + \nu$ (blue dot), and $\mu \rightarrow e + \gamma$ (magenta dot). Wave packet of another daughter is ∞ and that of the parent is $\sigma_{parent} m_\pi^2 = 10000$. The horizontal line shows the size of wave packets of the light particle in units of σm_π^2 and the vertical line shows the deviations of the rates for wave packets over the rates for the plane waves, $1 - \frac{P_{wave\ packet}}{P_{plane\ wave}}$. Errors for π and μ are slightly larger than others due to numerical uncertainty.

The parameter δ is not measured in the ordinary experiment and is integrated. From the integration over δ , we have

$$\int d\delta \prod_i d\vec{X}_{T,i} \frac{d\vec{p}_i}{(2\pi)^3} |\mathcal{M}|^2 = T \int \prod_i d\vec{X}_{T,i} \frac{d\vec{p}_i}{(2\pi)^3} \frac{\sum_l (v_l^2 - \vec{v}_l \cdot \vec{v}_A)}{\sqrt{\sum_l (\vec{v}_l - \vec{v}_A)^2}} |\mathcal{M}|^2. \quad (104)$$

Thus the probability in the system of finite σ_s and σ_t is proportional to time interval, T . Its magnitude is independent of the parameters of wave packet from the completeness Eq. (40) and agrees with the value obtained with $S[\infty]$ defined with plane waves combined with $i\epsilon$ prescription.

In Fig. (3), the rates computed with the wave packets of various sizes are compared with those of the plane waves in various decays, $J/\Psi \rightarrow M(2981) + \gamma$, $J/\Psi \rightarrow \eta(1409) + \gamma$, $\pi \rightarrow \mu + \nu$ and $\mu \rightarrow e + \gamma$ which will be discussed later. Wave packet of another daughter is ∞ and that of the parent is $\sigma_{parent} m_\pi^2 = 10000$. The value is the same for all processes. Within small errors, they agree.

4.3. Various cases of wave packets

We study the amplitude and probability of the systems (1) $\sigma_s = \text{finite}$, $\sigma_t = \text{finite}$, (2) $\sigma_s = \text{finite}$, $\sigma_t = \infty$, (3) $\sigma_s = \infty$, $\sigma_t = \infty$ in the following.

4.3.1. *Finite σ_s and finite σ_t .* When σ_A , σ_B , and σ_C are finite, σ_s and σ_t are also finite and the integrand in Eq. (90) decreases fast at $t \rightarrow \infty$ and $|\vec{x}| \rightarrow \infty$ and integrals over t and \vec{x} converge fast, and the results of Eqs. (50), (51) and (53) are applied. The total probability is obtained by integrating the momentum and position of Eq. (102), and does not have a finite-size correction at a macroscopic T.

When σ_A and σ_B are finite and $\sigma_C = \infty$, σ_t and σ_s are finite generally. We have

$$\frac{1}{\sigma_s} = \frac{1}{\sigma_A} + \frac{1}{\sigma_B}, \quad (105)$$

$$\frac{1}{\sigma_t} = \frac{(\vec{v}_A - \vec{v}_B)^2}{\sigma_A + \sigma_B}, \quad (106)$$

$$\vec{v}_0 = \sigma_s \left(\frac{\vec{v}_A}{\sigma_A} + \frac{\vec{v}_B}{\sigma_B} \right). \quad (107)$$

The integrand of Eq. (90) decreases fast at $|\vec{x} - \vec{x}_0| \rightarrow \infty$ and the integral over \vec{x} converges fast. σ_t is finite when $\vec{v}_A \neq \vec{v}_B$ and the integrand decreases fast at $|t - t_0| \rightarrow \infty$ and the integral over t converges fast. We have

$$R_{trajectory} = - \frac{\left\{ \left(\vec{X}_B - \vec{X}_A \right)_T \right\}^2}{2(\sigma_A + \sigma_B)}, \quad (108)$$

$$(\vec{X}_B - \vec{X}_A)_T = (\vec{X}_B - \vec{X}_A) - \frac{(\vec{v}_B - \vec{v}_A)}{|\vec{v}_B - \vec{v}_A|} \cdot (\vec{X}_B - \vec{X}_A) \frac{(\vec{v}_B - \vec{v}_A)}{|\vec{v}_B - \vec{v}_A|}.$$

Thus the probability depends on the transversal components of coordinate $\vec{X}_B - \vec{X}_A$ but not on the longitudinal component. The coordinate of B is integrated over the transversal and longitudinal components

$$\int d\vec{X}_B e^{2R_{trajectory}} = \int d(\vec{X}_B - \vec{X}_A)_T d(\vec{X}_B - \vec{X}_A)_L e^{2R_{trajectory}}, \quad (109)$$

where the former variables are integrated in the form:

$$\int d(\vec{X}_B - \vec{X}_A)_T e^{2R_{trajectory}} = \pi(\sigma_A + \sigma_B), \quad (110)$$

and the latter variable is integrated using $\theta(\vec{X}_i, T_i)$ in Eq. (90), as

$$\int d(\vec{X}_B - \vec{X}_A)_L = |\vec{v}_B - \vec{v}_A| \int d(T_B - T_A) = |\vec{v}_B - \vec{v}_A| T. \quad (111)$$

Thus the probability is proportional to T, and does not have the finite-size correction. $R_{momentum}$ is expressed with Eq. (97) or with the energies of the momenta

$$\vec{p}_A = \vec{p}_A - \frac{\sigma_B}{\sigma_A + \sigma_B} (\vec{p}_A - \vec{p}_B - \vec{p}_C), \quad (112)$$

$$\vec{p}_B = \vec{p}_B + \frac{\sigma_A}{\sigma_A + \sigma_B} (\vec{p}_A - \vec{p}_B - \vec{p}_C), \quad (113)$$

$$\vec{p}_C = \vec{p}_C. \quad (114)$$

Other cases of two wave packets and one plane wave are equivalent to the previous case.

In case of $\vec{v}_B = \vec{v}_A$;

In the limit $\vec{v}_B \rightarrow \vec{v}_A$, σ_t diverges and may cause a large diffraction effect. Nucleus trapped in matter have the momenta $\vec{p}_A = \vec{p}_B = 0$ and Mössbauer effect is such phenomenon that occurs through absorption of a gamma ray by a nucleus.

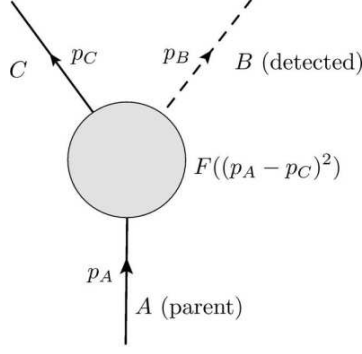


Fig. 4 Form factor in $\langle A|J_B(0)|C\rangle$.

4.3.2. Finite σ_s and infinite σ_t . In finite σ_s and infinite σ_t , the wave functions of initial and final states overlap in a long strip region, accordingly the probability shows unusual finite-size corrections.

A: Small mass

We study next the situation where the particle A and C are described by plane waves

$$\sigma_A = \infty, \sigma_C = \infty, \quad (115)$$

of the momenta \vec{p}_A and \vec{p}_C and B is described by the wave packet of the size σ_B and momentum \vec{p}_B . B is assumed to have a small mass m_B . A is prepared at T_A and B is detected at a space time position (\vec{X}_B, T_B) . Obviously the parameters of Eq. (46) become

$$\sigma_s = \sigma_B, \quad (116)$$

$$\vec{v}_0 = \vec{v}_B, \quad (117)$$

$$\frac{1}{\sigma_t} = \frac{\vec{v}_B^2}{\sigma_B} - \frac{\vec{v}_0^2}{\sigma_s} = 0. \quad (118)$$

Since $\sigma_t = \infty$, the integrand in probability does not decrease with t and may receive a finite-size correction.

The transition amplitude is expressed in the form,

$$\mathcal{M} = \int d^4x N_1 w_B(\vec{p}_B, \vec{x}) e^{-ip_A \cdot x + ip_C \cdot x} F((p_A - p_C)^2), \quad (119)$$

where $N_1 = ig(m_C m_B / E_C E_B)^{1/2}$ and the coefficient N_B in $w_B(\vec{p}_B, \vec{x})$ is $N_B = (\sigma_B / \pi)^{4/3}$, $F((p_A - p_C)^2)$ is the form factor, and the time t is integrated over the region $T_A \leq t \leq T_B$. σ_B is estimated using the size of a constituent object in a target which B interacts with. The coordinate \vec{x} is integrated next and the amplitude becomes finally

$$\begin{aligned} \mathcal{M} &= N_1 N_B (2\pi / \sigma_B)^{\frac{3}{2}} (4\pi \sigma_B)^{\frac{1}{2}} e^{-i(E_B T_B - \vec{p}_B \cdot \vec{X}_B)} e^{-\frac{\sigma_B}{2}(\vec{p}_A - \vec{p}_B - \vec{p}_C)^2} \\ &\quad \times \int_0^T dt e^{-i(E_A - E_C - E_B - (\vec{p}_A - \vec{p}_B - \vec{p}_C) \cdot \vec{v}_B)t} F((p_A - p_C)^2) \\ &= N_1 N_B (2\pi / \sigma_B)^{\frac{3}{2}} (4\pi \sigma_B)^{\frac{1}{2}} e^{-i(E_B T_B - \vec{p}_B \cdot \vec{X}_B)} e^{-\frac{\sigma_B}{2}(\vec{p}_A - \vec{p}_B - \vec{p}_C)^2} \\ &\quad \times F((p_A - p_C)^2) \frac{\sin(\omega T / 2)}{\omega} e^{i\omega T / 2}, \end{aligned} \quad (120)$$

where ω is

$$\omega = E_A - E_C - E_B - (\vec{p}_A - \vec{p}_B - \vec{p}_C) \cdot \vec{v}_B, \quad (121)$$

Because the magnitude is inversely proportional to ω , \mathcal{M} gets contributions from small and large ω regions. The amplitude gets a large contribution at a large T from the region,

$$\omega \approx 0. \quad (122)$$

A normal root of satisfying

$$E_A - E_C - E_B \approx 0, \quad \vec{p}_A - \vec{p}_B - \vec{p}_C \approx 0, \quad (123)$$

and a new root of satisfying

$$E_A - E_C - E_B \neq 0, \quad \vec{p}_A - \vec{p}_B - \vec{p}_C \neq 0, \quad (124)$$

exist. Because the kinetic energy and momentum are different from those of the initial state, the secondary root gives the finite-size correction due to the diffraction. Dependence of the amplitude on \vec{p}_B is determined by a root of $\omega = 0$ and its slope $\frac{\partial \omega}{\partial \vec{p}_B}$.

Assuming $|\vec{p}_A - \vec{p}_C - \vec{p}_B|$ is small, we have

$$E_B(\vec{p}_B) + (\vec{p}_A - \vec{p}_B - \vec{p}_C) \cdot \vec{v}_B = E_B(\vec{p}_A - \vec{p}_C), \quad (125)$$

and

$$\omega = E_A(\vec{p}_A) - E_C(\vec{p}_C) - E_B(\vec{p}_A - \vec{p}_C). \quad (126)$$

The probability integrated over \vec{p}_C becomes

$$\begin{aligned} & N_1^2 N_B^2 (2\pi/\sigma_B)^3 (4\pi\sigma_B) \int \frac{d\vec{p}_C}{(2\pi)^3} e^{-\sigma_B(\vec{p}_A - \vec{p}_B - \vec{p}_C)^2} \left(\frac{\sin(\omega T/2)}{\omega} \right)^2 F((p_A - p_C)^2) \\ & = N_1^2 N_B^2 (2\pi/\sigma_B)^3 (4\pi\sigma_B) \int d\omega \left(\frac{\sin(\omega T/2)}{\omega} \right)^2 \rho(\omega), \end{aligned} \quad (127)$$

where the spectrum density $\rho(\omega)$ is

$$\begin{aligned} \rho(\omega) &= \int \frac{d\vec{p}_C}{(2\pi)^3} e^{-\sigma_B(\vec{p}_A - \vec{p}_B - \vec{p}_C)^2} \\ &\quad \times \delta(\omega - E_A(\vec{p}_A) + E_C(\vec{p}_C) + E_B(\vec{p}_A - \vec{p}_C)) F((p_A - p_C)^2). \end{aligned} \quad (128)$$

Because $\rho(0)$ is finite and $\rho(\omega)$ decreases rapidly at the large ω region, as is given in Appendix A, the following integral converges at a finite T ,

$$\int d\omega \left(\frac{\sin(\omega T/2)}{\omega} \right)^2 \rho(\omega) = T \left\{ 2\pi\rho(0) + \frac{1}{T}\zeta \right\}, \quad (129)$$

where ζ is equal to $C(T)$ in Appendix A. Thus the finite-size correction becomes finite.

The finite-size correction to the total probability integrated over whole momentum region of \vec{p}_C is obtained easily with the correlation function [21],

$$\int \frac{d\vec{p}_C}{(2\pi)^3} |\mathcal{M}|^2 = \frac{N_2}{E_B} \int d^4x_1 d^4x_2 e^{-\frac{1}{2\sigma_B} \sum_i (\vec{x}_i - \vec{x}_i^0)^2} \Delta_{A,C}(\delta x) e^{i\phi(\delta x)}, \quad (130)$$

where $N_2 = g^2 (4\pi/\sigma_B)^{3/2} V^{-1}$, V is a normalization volume for the initial state A , $\vec{x}_i^0 = \vec{X}_B + \vec{v}_B(t_i - T_B)$, $\delta x = x_1 - x_2$, $\phi(\delta x) = p_B \cdot \delta x$ and

$$\Delta_{A,C}(\delta x) = \frac{1}{(2\pi)^3} \int \frac{d\vec{p}_C}{E(\vec{p}_C)} e^{-i(p_A - p_C) \cdot \delta x} F((p_A - p_C)^2). \quad (131)$$

In the right-hand side of Eq.(131), the integration region of the momentum \vec{p}_C is that of the complete set and is reduced to the smaller one if the integrand $|\mathcal{M}|^2$ vanishes in some

kinematical region. This happens for the amplitude of plane waves at the asymptotic region $T = \infty$, which includes the delta function, $\delta^{(4)}(\delta p)$, from the integration over x reflecting the conservation law of kinetic energy and momentum. The phase space of the final state becomes proportional to the initial energy, then. Now in the right-hand side of Eq. (131), the coordinates are fixed and are not integrated. Thus the correlation function $\Delta_{A,C}(\delta x)$ does not include $\delta^{(4)}(\delta p)$, and \vec{p}_c is integrated over the whole region..

Because the probability is finite, integration variables can be interchanged. For $\tilde{m}^2 = m_A^2 - m_C^2 \geq 0$ and a real p_A , [18, 19, 21], and from Appendix C,

$$\begin{aligned}\Delta_{A,C}(\delta x) &= 2i \left[F(-\tilde{m}^2) D_{\tilde{m}} \left(-i \frac{\partial}{\partial \delta x} \right) \left(\frac{\epsilon(\delta t)}{4\pi} \delta(\lambda) + f_{short} \right) + I_2 \right], \\ D_{\tilde{m}} \left(-i \frac{\partial}{\partial \delta x} \right) &= \sum_l \frac{1}{l!} \left(2p_{\pi} \cdot \left(-i \frac{\partial}{\partial \delta x} \right) \frac{\partial}{\partial \tilde{m}^2} \right)^l, \\ f_{short} &= -\frac{i\tilde{m}^2}{8\pi\xi} \theta(-\lambda) \{ N_1(\xi) - i\epsilon(\delta t) J_1(\xi) \} - \frac{i\tilde{m}^2}{4\pi^2\xi} \theta(\lambda) K_1(\xi),\end{aligned}\tag{132}$$

where $\epsilon(\delta t)$ is equal to $= +1$ or -1 for positive or negative δt , respectively, $\lambda = (\delta x)^2$, $\xi = \tilde{m}\sqrt{|\lambda|}$, and N_1 , J_1 , and K_1 are Bessel functions. f_{short} has a singularity of the form $1/\lambda$ around $\lambda = 0$ and decrease as $e^{-\tilde{m}\sqrt{|\lambda|}}$ or oscillates as $e^{i\tilde{m}\sqrt{|\lambda|}}$ at large $|\lambda|$. The condition for the convergence of the series will be studied later. The formula for A with a finite life-time is obtained later. The last term is

$$I_2 = \frac{1}{(2\pi)^3} \int F((p_A - p_C)^2) \theta(p_A^0 - p_C^0) \frac{d\vec{p}_C}{E(\vec{p}_C)} e^{-i(p_A - p_C) \cdot \delta x}.\tag{133}$$

For $\tilde{m}^2 = m_A^2 - m_C^2 < 0$,

$$\Delta_{A,C}(\delta x) = 0.\tag{134}$$

Thus $\Delta_{A,C}(\delta x)$ is composed of the light-cone singularity $\delta(\lambda)\epsilon(\delta t)$ [18, 32], the regular terms written by Bessel functions, and I_2 . The former two terms come from the integration from $E_A \leq E_C$, and are finite in a finite T . So using this expression the finite T correction which is unable to obtain with standard calculations of plane waves can be found. Because the integration region for this is outside of the kinematical region of conserving the energy and momentum, this integral vanishes at $T = \infty$ in fact. I_2 , on the other hand, comes from the region $E_C \leq E_A$, which is the kinematical region satisfying the energy and momentum conservation, determines the quantities at $T = \infty$. This expression of writing the probability with the light-cone singularity converges and is valid in the kinematical region $2p_A \cdot p_B \leq \tilde{m}_C^2$, where $\tilde{m}_C^2 = m_A^2 - m_C^2$.

Substituting the expression of $\Delta_{A,C}(\delta x)$ into Eq. (130) and integrating over \vec{x}_1 and \vec{x}_2 , we have

$$\begin{aligned}J_{\delta(\lambda)} &= \int d\vec{x}_1 d\vec{x}_2 e^{i\phi(\delta x)} e^{-\frac{1}{2\sigma_B} \sum_i (\vec{x}_i - \vec{X}_B - \vec{v}_B(t_i - T_B))^2} \frac{1}{4\pi} \delta(\lambda) \epsilon(\delta t) \\ &\approx (\sigma_B \pi)^{\frac{3}{2}} \frac{\sigma_B}{2} \frac{\epsilon(\delta t)}{|\delta t|} e^{i\bar{\phi}_c(\delta t)},\end{aligned}\tag{135}$$

for the leading singular part and

$$J_{1/\lambda} = \int d\vec{x}_1 d\vec{x}_2 e^{i\phi(\delta x)} e^{-\frac{1}{2\sigma_B} \sum_i (\vec{x}_1 - \vec{X}_B - \vec{v}_B(t_1 - T_B))^2} \frac{i}{4\pi^2 \lambda} \\ \approx (\sigma_B \pi)^{\frac{3}{2}} \frac{\sigma_B}{2} \left(\frac{1}{\pi \sigma_B |\vec{p}_B|^2} \right)^{\frac{1}{2}} e^{-\sigma_B |\vec{p}_B|^2} \frac{1}{|\delta t|} e^{i\bar{\phi}_c(\delta t)}, \quad (136)$$

for the next term of the form $1/\lambda$.

Finally we integrate t_1 and t_2 over the finite region $T = T_B - T_A$, and we have the slowly decreasing term $\tilde{g}(\omega_B T)$

$$i \int_0^T dt_1 dt_2 \frac{\epsilon(\delta t)}{|\delta t|} e^{i\omega_B \delta t} = T(\tilde{g}(\omega_B T) - \pi), \quad (137)$$

$$\omega_B = E_B - |\vec{p}_B| = \frac{m_B^2}{2E_B},$$

and the normal term G_0 . $\tilde{g}(\omega_B T)$ is generated from the light-cone singularity and related term and satisfies

$$\tilde{g}(0) = \pi, \quad (138)$$

$$\tilde{g}(\omega_B T) \rightarrow \frac{2}{\omega_B T}; \quad T \rightarrow \infty, \quad (139)$$

and vanishes at $T = \infty$. G_0 is from the rest

$$G_0 = 2\sqrt{\frac{\sigma_B}{\pi}} \int \frac{d\vec{p}_C}{E(\vec{p}_C)} \delta(E_A - E_B - E_C(\vec{p}_C)) e^{-\sigma_B (\vec{p}_A - \vec{p}_B - \vec{p}_C)^2} \theta(E_A - E_C(\vec{p}_C)), \quad (140)$$

and conserves the kinetic energy and momentum approximately

$$p_A - p_C = p_B, \quad (141)$$

and gives the asymptotic value. Due to the rapid oscillation in δt , G_0 gets contribution from the microscopic $|\delta t|$ region and is constant in T . Integration of this term does not depend on σ_B and agrees with the normal probability obtained with the standard method of using plane waves. In the region $2p_A \cdot p_B > \tilde{m}_C^2$, $\Delta_{A,C}(\delta x)$ does not have a light-cone singularity and the diffraction term exists only in the kinematical region $2p_A \cdot p_B \leq \tilde{m}_C^2$. This region depends upon the mass of C , hence the diffraction terms of all three mass eigenstates converge in the union of the kinematical regions of the three masses, $2p_A \cdot p_B \leq \tilde{m}_C^2$. The diffraction terms exists in this region.

We have

$$\int \frac{d\vec{p}_C}{(2\pi)^3} |\mathcal{M}|^2 = \frac{N_2}{E_B} \{ F(-\tilde{m}^2) \tilde{g}(\omega_B T) + F(m_B^2) G_0 \}, \quad (142)$$

where $N_2 = g^2 (4\pi/\sigma_B)^{3/2} V^{-1}$, V is a normalization volume for the initial state A . Form factor gives different corrections to the diffraction and normal terms. They are evaluated later.

B: massless particle $m_B = 0$

For a massless B , the leading singularity $\delta(\lambda)\epsilon(\delta t)$ cancels on integrating over the times and the next term proportional to $1/\lambda$ gives a dominant contribution. The integral of this

term

$$J_{1/\lambda} = \int d\vec{x}_1 d\vec{x}_2 e^{i\phi(\delta x)} e^{-\frac{1}{2\sigma_B} \sum_i (\vec{x}_1 - \vec{X}_B - \vec{v}_B(t_1 - T_B))^2} \frac{i}{4\pi^2 \lambda}, \quad (143)$$

leads

$$J_{1/\lambda} \approx (\sigma_B \pi)^{\frac{3}{2}} \frac{\sigma_B}{2} \left(\frac{1}{\pi \sigma_B |\vec{p}_B|^2} \right)^{\frac{1}{2}} e^{-\sigma_B |\vec{p}_B|^2} \frac{1}{|\delta t|}. \quad (144)$$

This term also has the universal dependence on $|\delta t|$ and its integration over the times becomes,

$$\int dt_1 dt_2 J_{1/\lambda} = (\sigma_B \pi)^{\frac{3}{2}} \frac{\sigma_B}{2} \left(\frac{1}{\pi \sigma_B |\vec{p}_B|^2} \right)^{\frac{1}{2}} e^{-\sigma_B |\vec{p}_B|^2} \int dt_1 dt_2 \frac{1}{|t_1 - t_2|}. \quad (145)$$

The integration over the times in a finite region from ϵ to T is

$$\int_{\epsilon}^T dt_1 dt_2 \frac{1}{|t_1 - t_2|} = T \left(2 \log \frac{T}{\epsilon} - 1 \right), \quad (146)$$

and

$$\int dt_1 dt_2 J_{1/\lambda} = (\sigma_B \pi)^{\frac{3}{2}} \frac{\sigma_B}{2} \left(\frac{1}{\pi \sigma_B |\vec{p}_B|^2} \right)^{\frac{1}{2}} e^{-\sigma_B |\vec{p}_B|^2} T \left(2 \log \frac{T}{\epsilon} - 1 \right). \quad (147)$$

This term gives the probability

$$P_{diff} = N_3 \int dp_B e^{-\sigma_B |\vec{p}_B|^2}, \quad (148)$$

where

$$N_3 = 8Tg^2 \left(\frac{\sigma_B^2}{4} \right) \left(2 \log \frac{T}{\epsilon} - 1 \right). \quad (149)$$

Large time: $T > \tau_A$

If T is larger than the life time of A , τ_A , Eqs. (138) and (146) are replaced with

$$i \int_0^T dt_1 dt_2 \frac{\epsilon(\delta t)}{|\delta t|} e^{i\omega_B \delta t} e^{-\frac{t_1+t_2}{\tau_A}} = \tilde{g}(\omega_B, T; \tau_A) - \tilde{g}(\omega_B, T; \tau_A), \quad (150)$$

$$\tilde{g}_\tau(\omega_B, \infty; \tau_A) = 0, \quad \omega_B = E_B - |\vec{p}_B| = \frac{m_B^2}{2E_B},$$

and

$$\int_{\epsilon}^T dt_1 dt_2 \frac{1}{|t_1 - t_2|} e^{-\frac{t_1+t_2}{\tau_A}}. \quad (151)$$

N_3 becomes approximately

$$N_3 = 8\tau_A g^2 \frac{\sigma_B^2}{4} \left(2 \log \frac{\tau_A}{\epsilon} - 1 \right). \quad (152)$$

Thus, the system of $\sigma_t = \infty$ has the finite-size correction of the form Eq. (142) for $T \ll \tau_A$, and $\tilde{g}(T\omega_B)$ in Eq. (142) is replaced with $\tilde{g}(T, \omega_B; \tau_A)$ in $T \approx \tau_A$. The correction depends on T in the universal manner and on the size of wave packet in magnitude. At $\sigma_B = \infty$, the correction becomes infinite.

We compute the total probability next. From the integration over \vec{X}_B , the total volume V is obtained and cancelled with the normalization of A . The total probability, then, becomes the integral of a sum of G_0 and $\tilde{g}(\omega_B T)$,

$$P = \begin{cases} N_3 \int \frac{d^3 p_B}{(2\pi)^3 E_B} [F(-\tilde{m}^2) \tilde{g}(\omega_B T) + F(m_B^2) G_0], & \text{for } T \ll \tau_A, \\ N_3 \int \frac{d^3 p_B}{(2\pi)^3 E_B} [F(-\tilde{m}^2) \tilde{g}(T, \omega_B; \tau_A) + F(m_B^2) G_0], & \text{for } \tau_A \leq T, \end{cases} \quad (153)$$

where $N_3 = 8Tg^2\sigma_B$. The second terms, P_{normal} , in the right-hand sides of the Eq. (153) are independent of T and σ_B and agree with the standard value computed with the plane waves. $\tilde{g}(\omega_B T)$ and $\tilde{g}(T, \omega_B; \tau_A)$ in the first terms depend on ω_B and T , and are corrections due to the finite distance between the initial and final states. Their magnitudes of the first terms, $P_{diffraction}$, at $T \rightarrow \infty$, are proportional to

$$P_{diffraction} = \tilde{N} F(-\tilde{m}^2) \frac{\sigma_B}{\omega_B T} = \tilde{N} F(-\tilde{m}^2) \frac{\sigma_B E_B}{m_B^2 T}, \quad (154)$$

where \tilde{N} is constant. $P_{diffraction}$ becomes significant for large $(\sigma_B E_B)/m_B^2$, i.e., small mass or large wave packet.

4.3.3. Infinite σ_s and infinite σ_t . When three particles are plane waves, $\sigma_s = \sigma_t = \infty$, the scattering amplitude and cross section are the standard one if $H_{int}(t)e^{-\epsilon|t|}$ is used. The space-time coordinates (t, \vec{x}) are integrated over the whole region and the energy and momentum are strictly conserved. The asymptotic values thus obtained with $S[\infty]$

$$\mathcal{M} = (2\pi)^4 g \delta^{(4)}(p_A - p_B - p_C) f, \quad (155)$$

$$P = g^2 |f|^2 \times (phase \ space), \quad (156)$$

agree with the asymptotic values obtained with $S[T]$. If the convergence factor $e^{-\epsilon|t|}$ is absent, the limit $T \rightarrow \infty$ is not unique and is consistent with the diverging correction in $\sigma_B \rightarrow \infty$ of the previous case.

4.3.4. Coherence length. The coherence length found from the amplitude of the initial and final states expressed with wave packets is finite. From Eq. (91), the integral in \vec{x} converges for a finite σ_s and that in t converges for a finite σ_t . σ_t becomes infinite with $\vec{v}_A = \vec{v}_B$ and $\sigma_C = \infty$, or $\sigma_A = \sigma_B = \infty$. In the latter case, the coherence length is $\hbar E_C / (m_C^2 c^3)$.

4.3.5. Asymmetric wave packets. For the asymmetric wave packets, the integral over (t, \vec{x}) is expressed by

$$\int dt \int d\vec{x} e^{-\frac{1}{2\sigma_s^L}(\vec{x}_L - \vec{x}_0^L)^2 - \frac{1}{2\sigma_s^T}(\vec{x}_T - \vec{x}_0^T)^2 - \frac{1}{2\sigma_t}(t - t_0)^2}, \quad (157)$$

where the sizes of the Gaussian exponents and other parameters are given by complicated expressions. Experiments of $\delta E \ll |\delta \vec{p}|$ are studied with the asymmetric wave packets.

5. Emission and absorption of light

Radiative transitions of particles

$$\begin{aligned} A &\rightarrow C + \gamma, \\ A + \gamma &\rightarrow C, \end{aligned} \tag{158}$$

expressed with wave packets are studied in various parameter regions. Electromagnetic interaction is expressed with

$$H_{int} = e \int d\vec{x} J_\mu(x) \mathcal{A}^\mu(x), \tag{159}$$

where $\mathcal{A}_\mu(x)$ is a photon field and $J_\mu(x)$ is a electromagnetic current. A matrix element of the current between eigen states of energy and momentum are written as

$$\langle C; p_C | J_\mu(x) | A; p_A \rangle = e^{i(p_A - p_C) \cdot x} \langle C; p_C | J_\mu(0) | A; p_A \rangle, \tag{160}$$

where

$$\langle C; p_C | J_\mu(0) | A; p_A \rangle = \Gamma_\mu F((p_A - p_C)^2), \tag{161}$$

with the form factor $F((p_A - p_C)^2)$ and the spin dependent factor, Γ_μ . We assume one form factor for simplicity, but it is straightforward to extend to a case of many form factors. In the normal term of the radiative transition, the energy-momentum is conserved, and

$$F((p_A - p_C)^2) = F(k_\gamma^2) = F(0), \tag{162}$$

hence the coupling strength is determined by $F(0)$.

In detectors, fundamental processes of a photon are, photo-electric effect, Compton effect, or e^+e^- pair production. Wave packet sizes of the photon, σ_γ , are nuclear sizes for the pair production due to nuclear electric field or atomic sizes or larger for the photo-electric effect and Compton effect, depending on the energy.

5.1. Universal background

The transition probabilities of radiative processes receive the finite-size corrections under certain situations and their energy spectra are modified by pseudo-Doppler effects. Since the finite-size correction is caused by the states that violate the conservation law of kinetic energy and momentum, the corresponding events look like backgrounds even though they are produced dynamically. They have universal properties and magnitudes that depend on the experimental apparatus.

5.1.1. Universal background. The universal background derived from the finite-size correction resulted from

$$\left| \frac{e^{i\omega T} - 1}{\omega} - 2\pi\delta(\omega) \right| \neq 0, \tag{163}$$

is inevitable consequence of Schödinger equation. Since they are generated by the states of the kinetic energy different from that of the initial state, that is positive semi-definite from Eq. (35) and is added to the normal component in the wave zone. Its magnitude is computed rigorously in relativistic systems Eq. (153). The correction vanishes in the particle zone. Energy spectrum for wave packets is distorted in both particle and wave zones due to the pseudo-Doppler effects even though the total probability agrees with the normal value.

5.1.2. *Form factor*. Nucleus, atom, and molecule are composite states and have internal structures. So they have finite extensions and interact with photon or neutrino non-locally. This non-locality is negligible if the size R and the photon momentum k_γ satisfies $k_\gamma R \ll 1$, where the multi-pole expansions are applicable.

For X-rays from atoms, they are about

$$k_\gamma R = 10^{-3}; \quad k_\gamma \sim \text{keV}, \quad R = 10^{-11} \text{ [m]}, \quad (164)$$

and for transitions of nucleus

$$k_\gamma R = 10^{-1}; \quad k_\gamma \sim \text{MeV}, \quad R = 10^{-15} \text{ [m]}. \quad (165)$$

Since $k_\gamma R$ is small,

$$F((p_A - p_C)^2) = F(0). \quad (166)$$

5.1.3. *Life time effect*. If the parent A has a finite life time, τ_A , that modifies the results. In a region

$$c\tau_A \leq \sqrt{\sigma_A}, \quad (167)$$

the integral over the times in the transition probability gets a dominant contribution from the region

$$t \leq \tau_A. \quad (168)$$

Then the effect of the wave packet is diminished and the pseudo-Doppler effect becomes negligible. If the life time satisfies

$$c\tau_A \geq \sqrt{\sigma_A}, \quad (169)$$

the integral over the times in the transition probability gets a dominant contribution from the region

$$t \leq \frac{\sqrt{\sigma_A}}{c}, \quad (170)$$

and the pseudo-Doppler effect is prominent.

5.1.4. *Photon effective mass*. Photon is massless in vacuum but its property is modified in matter due to dielectric constant. In high-energy regions, the refraction constant behaves with the frequency as

$$n = 1 - \frac{\omega_p^2}{\omega^2}, \quad (171)$$

where ω_p is the plasma frequency and is given as

$$\omega_p^2 = \frac{NZe^2}{\epsilon_0 m_e}, \quad (172)$$

depends on material, density, and other parameters. The wave vector satisfies

$$(ck)^2 = \omega^2 - \omega_p^2, \quad (173)$$

and the energy dispersion becomes

$$\vec{p} = E(\vec{p})^2 - (\hbar\omega_p)^2. \quad (174)$$

Thus the photon has an effective mass

$$m_{eff} = \hbar \sqrt{\frac{NZe^2}{\epsilon_0 m_e}}, \quad (175)$$

where N and Z are a number density and atomic number of gas, and m_e is the electron's mass. The m_{eff} depends upon the density of matter and varies. The high-energy photon behaves like a massive particle.

5.1.5. Light-cone singularity for general systems. For particles A and C of internal structures, Eq. (161) is substituted to Eq. (131). As is shown in Appendix C, the singular part of correlation function is written in the form,

$$\Delta_{A,C}(\delta x)^{light-cone} = F(-m_A^2 + m_C^2) \Delta_{A,C}^{(0),light-cone}(\delta x), \quad (176)$$

where $\Delta_{A,C}^{(0)}(\delta x)$ is that of the point particle. Thus the form factor

$$F(m_C^2 - m_A^2), \quad (177)$$

determines the strength of the singularity and are given in Appendix C, as

$$F(m_C^2 - m_A^2)/F(0) = \begin{cases} O(1); & \text{hadron, positronium, light nucleus,} \\ O(10^{-1}); & \mu N \text{ atom, heavy nucleus,} \\ O(10^{-5}); & \mu e, K - \text{electron,} \\ O(10^{-10}); & \text{atom,} \end{cases} \quad (178)$$

Thus the form factors do not modify the magnitude of light-cone singularity for hadrons, light nucleus, positronium, and reduce to 1/10 for μ -N atom and heavy molecules. For μ -e, K-electron, and atoms, the magnitudes become extremely small. Eq. (177) is almost the same as the on-shell coupling, Eq. (162) in the former but much smaller in the latter. Because the singularity is caused by the waves of translational motion which retain the relativistic invariance even for the particles with internal structure, but the magnitude depends on their sizes.

5.2. Emission of lights

5.2.1. Decay in flight in vacuum. 1. Finite σ_A and σ_γ : pseudo-Doppler effect

The amplitude of a radiative decay of A to C and a photon γ of momenta, positions and wave packet sizes

$$\begin{aligned} A &: (\vec{X}_A, E_A, \vec{p}_A, \sigma_A), \\ \gamma &: (\vec{X}_\gamma, E_\gamma, \vec{p}_\gamma, \sigma_\gamma), \quad E_\gamma^2 - \vec{p}_\gamma^2 = 0, \\ C &: (\vec{p}_C, E_C, \sigma_C = \infty), \end{aligned} \quad (179)$$

is expressed with the matrix element of the current operator and the photon field

$$\begin{aligned} \mathcal{M} &= \int d^4x \langle C | J_\mu(x) | A \rangle \langle \gamma | \mathcal{A}^\mu(x) | 0 \rangle \\ &= \int d^4x e^{i(p_A - p_C - p_\gamma) \cdot x} F_{AB} e^{ip_\gamma \cdot X_\gamma - \frac{1}{2\sigma_\gamma} (\vec{x} - \vec{X}_\gamma - \vec{v}_\gamma(t - T_\gamma))^2} \\ &\quad \times e^{-ip_A \cdot X_A - \frac{1}{2\sigma_A} (\vec{x} - \vec{X}_A - \vec{v}_A(t - T_A))^2} = e^{R+i\phi}, \\ F_{AB} &= \langle C | J_\mu(0) | A \rangle \epsilon^\mu(\vec{p}_\gamma), \end{aligned} \quad (180)$$

where $\epsilon^\mu(\vec{k}_\gamma)$ is a polarization vector of the photon. We have $|\mathcal{M}|^2$ in the form

$$|\mathcal{M}|^2 = N^2 \int dx_1 dx_2 e^{i(p_A - p_C - p_\gamma) \cdot (x_1 - x_2) - \frac{1}{2\sigma_\gamma} \sum (\vec{x}_i - \vec{X}_\gamma - \vec{v}_\gamma(t_i - T_\gamma))^2} \\ \times e^{-\frac{1}{2\sigma_A} \sum (\vec{x}_i - \vec{X}_A - \vec{v}_A(t_i - T_A))^2} W_{i,j}(p_A, p_C) (\delta^{i,j} - \frac{p_\gamma^i p_\gamma^j}{\vec{p}_\gamma^2}), \quad (181)$$

in Coulomb gauge,

$$\mathcal{A}_0(x) = 0, \quad \nabla \cdot \vec{\mathcal{A}}(x) = 0, \quad (182)$$

where N is the normalization factor, and

$$W_{i,j}(p_A, p_C) = \langle C | J_i(0) | A \rangle (\langle C | J_j(0) | A \rangle)^*, \quad (183)$$

$$(\delta^{i,j} - \frac{p_\gamma^i p_\gamma^j}{\vec{p}_\gamma^2}) = \sum \epsilon^i(\vec{k}_\gamma) (\epsilon^j(\vec{k}_\gamma))^*. \quad (184)$$

R in Eq.(180) is composed of the momentum-dependent part $R_{momentum}$ and the coordinate-dependent part $R_{trajectory}$. The former is

$$R_{momentum} = -\frac{\sigma_t}{2} (E_A(\vec{p}_A) - E_C(\vec{p}_C) - E_\gamma(\vec{\tilde{p}}_\gamma))^2 - \frac{\sigma_s}{2} (\vec{p}_A - \vec{p}_C - \vec{p}_\gamma)^2, \\ \vec{\tilde{p}}_\gamma = \vec{p}_\gamma + \frac{\sigma_s}{\sigma_\gamma} (\vec{p}_A - \vec{p}_C - \vec{p}_\gamma), \quad (185)$$

where σ_s , σ_t and \vec{v}_0 are

$$\sigma_s = \frac{\sigma_A \sigma_\gamma}{\sigma_A + \sigma_\gamma}, \quad (186)$$

$$\vec{v}_0 = \frac{\sigma_A}{\sigma_A + \sigma_\gamma} \vec{v}_\gamma, \quad (187)$$

$$\frac{1}{\sigma_t} = \frac{\vec{v}_\gamma^2}{\sigma_\gamma} - \frac{\vec{v}_0^2}{\sigma_s} = \frac{\vec{v}_\gamma^2}{\sigma_A + \sigma_\gamma}. \quad (188)$$

Thus, the energy-momentum satisfies the modified conservation law. The momentum is conserved approximately around the center $\delta\vec{p} = 0$, whereas the photon's energy at the momentum $\vec{\tilde{p}}_\gamma$ fulfills the approximate conservation law. Implications will be studied in detail shortly.

The position-dependent exponent is written in the form:

$$R_{trajectory} = -\frac{\vec{X}_A^2}{2\sigma_A} - \frac{\vec{\tilde{X}}_\gamma^2}{2\sigma_\gamma} + 2\sigma_s \left(\frac{\vec{X}_A}{2\sigma_A} + \frac{\vec{\tilde{X}}_\gamma}{2\sigma_\gamma} \right)^2 \\ + 2\sigma_t \left(\frac{\vec{v}_0 \cdot \vec{X}_A}{2\sigma_A} + \frac{(\vec{v}_0 - \vec{v}_\gamma) \cdot \vec{\tilde{X}}_\gamma}{2\sigma_\gamma} \right)^2 \\ = -\frac{1}{2(\sigma_A + \sigma_\gamma)} \left[(\vec{X}_A - \vec{\tilde{X}}_\gamma)^2 - \frac{1}{v_\gamma^2} (\vec{v}_\gamma \cdot (\vec{X}_A - \vec{\tilde{X}}_\gamma))^2 \right]. \quad (189)$$

The probability is expressed as

$$\begin{aligned}
P &= N^2 \exp(2R_{momentum} + 2R_{trajectory}) |F_{A,B}|^2 \\
&= N^2 |F_{A,B}|^2 \exp \left[-\sigma_t (E_A - E_\gamma(\tilde{\vec{p}}_\gamma) - E_C)^2 - \sigma_s (\vec{p}_A - \vec{p}_C - \vec{p}_\gamma)^2 \right] \\
&\quad \times \exp \left[-\frac{(\vec{X}_A - \vec{X}_\gamma)_T^2}{\sigma_A + \sigma_\gamma} \right], \tag{190}
\end{aligned}$$

and has no finite-size correction. Thus the total probability agrees to that of plane waves. Nevertheless, the energy spectrum of Eq. (190) is distorted due to pseudo-Doppler effect. The photon's momentum is distributed around a center $\vec{p}_A - \vec{p}_C$ and the photon's energy at a momentum $\tilde{\vec{p}}_\gamma$ is distributed around $E_A - E_C$. If σ_s is small and σ_t is large, the momentum distribution is wide but the energy $E(\tilde{\vec{p}}_\gamma)$ coincides almost with $E_A - E_C$. The observed photon's energy is $E_\gamma(\vec{p}_\gamma)$ and is given from Eq. (185)

$$\begin{aligned}
E_\gamma(\vec{p}_\gamma) &= E_\gamma(\tilde{\vec{p}}_\gamma - \frac{\sigma_s}{\sigma_\gamma}(\vec{p}_A - \vec{p}_C - \vec{p}_\gamma)) \\
&= E_A - E_C - \frac{\sigma_s}{\sigma_\gamma} \vec{v}_\gamma \cdot (\vec{p}_A - \vec{p}_C - \vec{p}_\gamma). \tag{191}
\end{aligned}$$

Thus $E_\gamma(\vec{p}_\gamma)$ is very different from $E_A - E_C$.

Photon is on mass shell and satisfies

$$E(\vec{p}_\gamma)^2 - \vec{p}_\gamma^2 = 0. \tag{192}$$

In an event where the energy-momenta (E_A, \vec{p}_A) , (E_C, \vec{p}_C) , and $(E_\gamma, \vec{p}_\gamma)$ are measured, and the momenta satisfy

$$\vec{p}_\gamma \neq \vec{p}_A - \vec{p}_C, \tag{193}$$

the photon's energy at the momentum $\tilde{\vec{p}}_\gamma$ satisfies

$$E_A - E_C = E_\gamma(\tilde{\vec{p}}_\gamma). \tag{194}$$

Consequently the mass shell condition at $\tilde{\vec{p}}_\gamma$

$$E_\gamma(\tilde{\vec{p}}_\gamma)^2 - \tilde{\vec{p}}_\gamma^2 = (E_A - E_C)^2 - \tilde{\vec{p}}_\gamma^2 = 0, \tag{195}$$

is satisfied. Substituting $\tilde{\vec{p}}_\gamma$, we have

$$(E_A - E_C)^2 - (\vec{p}_\gamma + \frac{\sigma_s}{\sigma_\gamma}(\vec{p}_A - \vec{p}_C - \vec{p}_\gamma))^2 = 0, \tag{196}$$

which gives a relation of the energies and momenta with the ratio σ_s/σ_γ . Measuring the energies and momenta, the ratio σ_s/σ_γ will be determined.

In a situation of

$$\sigma_\gamma \ll \sigma_A, \quad (197)$$

we have

$$\sigma_s = \sigma_\gamma, \quad \sigma_t = \sigma_A, \quad \sigma_s \ll \sigma_t, \quad (198)$$

$$\vec{v}_0 = \frac{\sigma_A}{\sigma_A + \sigma_\gamma} \vec{v}_\gamma, \quad \tilde{\vec{p}}_\gamma = \frac{\sigma_\gamma}{\sigma_A + \sigma_\gamma} \vec{p}_\gamma + (\vec{p}_A - \vec{p}_C). \quad (199)$$

The central values of energies and momenta satisfy

$$\langle E_\gamma(\tilde{\vec{p}}_\gamma) \rangle = \langle E_A - E_C \rangle, \quad (200)$$

$$\langle \vec{p}_\gamma \rangle = \langle \vec{p}_A - \vec{p}_C \rangle, \quad (201)$$

with variations

$$\delta E = \frac{1}{\sqrt{\sigma_t}}, \quad (202)$$

$$|\delta \vec{p}| = \frac{1}{\sqrt{\sigma_s}}, \quad (203)$$

The energy spreading is narrower than the momentum spreading,

$$\delta E \ll |\delta \vec{p}|, \quad (204)$$

hence the constraint to the energy is more stringent than that of the momentum.

Heavy A and C (Pseudo-Doppler effect combined with Mössbauer effect)

If C and A are a ground state and an excited state of a heavy atom which bound together to become massive objects, the correlation function of Eq. (183) does not vanish only at the same momenta,

$$\vec{p}_A = \vec{p}_C, \quad (205)$$

like those of Mössbauer effect. We study the photon's energy spectrum when this condition is satisfied in a large wave packet $\sigma_A = \sigma_C$. The reduced momentum becomes

$$\tilde{\vec{p}}_\gamma = \frac{\sigma_\gamma}{\sigma_A + \sigma_\gamma} \vec{p}_\gamma, \quad (206)$$

from Eq. (198). The energy of the massless particle is proportional to the momentum and

$$\langle E_\gamma(\tilde{\vec{p}}_\gamma) \rangle = \frac{\sigma_\gamma}{\sigma_A + \sigma_\gamma} \langle E_\gamma(\vec{p}_\gamma) \rangle, \quad (207)$$

Substituting Eq. (200), we have the expectation value of E_γ

$$\langle E_\gamma(\vec{p}_\gamma) \rangle = \kappa \Delta E_{\text{electron}}, \quad (208)$$

$$\kappa = \frac{\sigma_A + \sigma_\gamma}{\sigma_\gamma}, \quad \Delta E_{\text{electron}} = E_A - E_C, \quad (209)$$

which is much larger than the energy difference $E_A - E_C$. Thus the product of average energy with the time interval for the light is equal to that for the atom

$$\sigma_\gamma \langle E_\gamma(\vec{p}_\gamma) \rangle = (\sigma_A + \sigma_\gamma)(E_A - E_C). \quad (210)$$

Now, σ_γ is the size of particle which the photon interacts with and σ_A is that of the atom, they are proportional to the average-time intervals of their reactions. Thus the conservation

law Eq. (62) for the energy is satisfied for average value. This unusual phenomenon occurs because the electromagnetic interaction takes place in the narrow space-time region where the wave functions of the A , C and photon overlap. When σ_γ is much smaller than σ_A , the region has the area σ_γ and moves with the velocity \vec{v}_γ furthermore. Hence the energy is conserved in this moving frame where the photon has the effective energy $E_\gamma(\vec{p}_\gamma)$, which is much smaller than $E_\gamma(\vec{p}_\gamma)$. Hence the average energy of γ becomes much larger than the energy difference between A and C . This is the pseudo-Doppler effect caused by the wave packets.

The condition, Eq. (197), is fulfilled in various situations. A molecule in gas propagates almost freely and an atom is bound in solid. The wave packet size of a molecule in gas is given by the square of mean free path and is of order of $10^{-14} [\text{m}^2]$, whereas that is the atomic distance in a solid of the order of $10^{-20} [\text{m}^2]$. Hence we have

$$\kappa = \frac{\sigma_A}{\sigma_\gamma} = 10^6. \quad (211)$$

Consequently the photon in this situation interacts with the atom in solid with the energy $\kappa \Delta E_{\text{electron}}$. For $\Delta E_{\text{electron}} = 0.1 [\text{eV}]$, E_γ can be as large as $100 [\text{keV}]$. Various anomalous luminescence of X-rays or γ -rays [33–35] may be connected with this energy enhancement.

For a photon produced from excited atom in solid and interacts with a nucleus in a solid, we have $10^{-20} [\text{m}^2]$ for the former size and $10^{-28} [\text{m}^2]$ for the latter size, and

$$\kappa = \frac{\sigma_A}{\sigma_\gamma} \approx O(10^8). \quad (212)$$

Consequently the photon produced from excited atoms interacts with a nucleus with much larger energy than the energy difference $\Delta E_{\text{electron}} = E_A - E_C$. Because the photon-Nucleus cross-section is much smaller than that of the photon-atom scattering, the probability of this event is extremely small.

A similar phenomenon is expected when charged particles propagate in magnetic field. A plane wave of the charge q and mass M in the magnetic field \vec{B}

$$e^{-i(E(\vec{p}_0) + \frac{q\vec{x} \times \vec{B}}{2M} \cdot \vec{p}_0)(t - T_0) + i\vec{p}_0 \cdot \vec{x}}, \quad (213)$$

has the phase proportional to Cyclotron frequency

$$\omega = \frac{q|\vec{B}|}{M}. \quad (214)$$

These waves behave like plane waves in a time region less than $T_i = \frac{2\pi}{\omega_i}$. T_i for the electron and proton are

$$T_i = \frac{2\pi}{\omega_i} = \frac{M_i}{q|\vec{B}|}, \quad i = e, p. \quad (215)$$

Thus the waves have the different sizes and its ratio is

$$\frac{T_e}{T_p} = \frac{m_e}{m_p} = \frac{1}{2000}. \quad (216)$$

Thus, the photon emitted from the atom interacts with the electron in a magnetic field can reveal the same energy enhancement.

The anomalous enhancement of the photon's energy results from the overlap of wave functions of different sizes. They occur when the photon's wave packets, which are the sizes

of the wave functions with which the photons interact, are much smaller than the parent's wave functions. Hence, the rate of the events may be quite low.

2. Infinite σ_A and finite σ_γ :finite-size correction

The amplitude of a radiative decay of A to C of plane waves and a γ of momenta, positions and wave packet sizes

$$\begin{aligned} A &: (\vec{X}_A, E_A, \vec{p}_A, \sigma_A = \infty), \\ \gamma &: (\vec{X}_\gamma, E_\gamma, \vec{p}_\gamma, \sigma_\gamma), \quad E_\gamma^2 - \vec{p}_\gamma^2 = 0 \\ C &: (\vec{p}_C, E_C, \sigma_C = \infty), \end{aligned} \quad (217)$$

is expressed with the matrix element of the current operator and the photon field

$$\begin{aligned} \mathcal{M} &= e \int d^4x \langle C | J_\mu(x) | A \rangle \langle \gamma | \mathcal{A}^\mu(x) | 0 \rangle \\ &= e \int d^4x e^{i(p_A - p_C - p_\gamma) \cdot x} \langle C | J_\mu(0) | A \rangle \epsilon^\mu(\vec{k}_\gamma) e^{ip_\gamma \cdot X_\gamma - \frac{1}{2\sigma_\gamma} (\vec{x} - \vec{X}_\gamma - \vec{v}_\gamma(t - T_\gamma))^2} \\ &= e^{R+i\phi}. \end{aligned} \quad (218)$$

We have $|\mathcal{M}|^2$ in the form

$$\begin{aligned} |\mathcal{M}|^2 &= N^2 \int d^4x_1 d^4x_2 e^{i(p_A - p_C - p_\gamma) \cdot (x_1 - x_2) - \frac{1}{2\sigma_\gamma} \sum (\vec{x}_i - \vec{X}_\gamma - \vec{v}_\gamma(t_i - T_\gamma))^2} \\ &\quad \times W_{i,j}(p_A, p_C) (\delta^{i,j} - \frac{p_\gamma^i p_\gamma^j}{\vec{p}_\gamma^2}). \end{aligned} \quad (219)$$

Integrating over \vec{p}_C with a variable $r = p_A - p_C$, we have

$$\begin{aligned} &\int \frac{d\vec{p}_C}{(2\pi)^3 E_C} e^{i(p_A - p_C) \cdot (x_1 - x_2)} W_{i,j}(p_A, p_C) \\ &= \int \frac{d^4r}{(2\pi)^3} \text{Im} \left[\frac{1}{r^2 - 2p_A \cdot r + m_A^2 - m_C^2 - i\epsilon} \right] W_{i,j}(p_A, p_A - r) e^{ir \cdot (x_1 - x_2)}, \end{aligned} \quad (220)$$

which has the light-cone singularity

$$\frac{i}{2\pi} \delta(\lambda) \epsilon(t_1 - t_2) W_{i,j}(p_A, p_A - r) |_{r^2 = m_C^2 - m_A^2}, \quad (221)$$

from the integration over the momentum $r = (r^0, \vec{r})$ of the region

$$r_0^2 - \vec{r}^2 = m_C^2 - m_A^2 < 0, \quad r^0 \leq 0. \quad (222)$$

It is noted that $|(p_A - p_C)^2| = |m_C^2 - m_A^2|$ is small and $|W_{i,j}(p_A, p_A - r)|$ is almost the same as the on-shell matrix element of the radiative transition. Eq. (220) has also regular terms and one of them is generated from the above kinematical region and the other terms are from the region $0 \leq r^0 \leq p_A^0$. The latter coincides with the normal term of the decay probability.

Thus we have

$$\int \frac{d^3 p_C}{E_C} |\mathcal{M}|^2 = P_{normal} + P_{diffraction}, \quad (223)$$

$$P_{diffraction} = \mathcal{C} \tilde{g}(\omega_\gamma T), \quad \omega_\gamma = \frac{m_{eff}^2}{2E_\gamma},$$

where \mathcal{C} is determined by the wave packet size. From the convergence condition in the expansion Eq. (220), the light-cone singularity exists in the momentum region

$$2p_A \cdot q \leq m_A^2 - m_C^2. \quad (224)$$

5.2.2. Decay at rest in solid . A decay of A in solid to C and a photon γ , which have momenta, positions and wave packet sizes

$$\begin{aligned} A &: (\vec{X}_A, E_A, \vec{p}_A = 0, \sigma_A), \\ \gamma &: (\vec{X}_\gamma, E_\gamma, \vec{p}_\gamma, \sigma_\gamma = \infty), \\ C &: (\vec{X}_C, \vec{p}_C = 0, E_C, \sigma_C), \end{aligned} \quad (225)$$

is a kinematical region of Mössbauer effect. The amplitude

$$\mathcal{M}(A \rightarrow C + \gamma) = g \int d^4 x w_A(\vec{p}_A = 0, x) w_C(\vec{p}_C = 0, x) e^{ip_\gamma \cdot x}, \quad (226)$$

where

$$w_A = N_A \left(\frac{2\pi}{\sigma_A} \right)^{\frac{3}{2}} e^{-\frac{1}{2\sigma_A} (\vec{x} - \vec{x}_A^0)^2 - i\phi_0^A}, \quad (227)$$

$$w_C = N_C \left(\frac{2\pi}{\sigma_C} \right)^{\frac{3}{2}} e^{-\frac{1}{2\sigma_C} (\vec{x} - \vec{x}_C^0)^2 - i\phi_0^C}, \quad (228)$$

$$\vec{x}_A^0 = \vec{X}_A, \quad \phi_0^A = m_A(t - T_A), \quad \vec{x}_C^0 = \vec{X}_C, \quad \phi_0^C = m_C(t - T_C),$$

is given as

$$\begin{aligned} \mathcal{M}(A \rightarrow C + \gamma) &= N e^{im_A T_A - m_C T_C} \int_0^T dt e^{-i(m_A - m_C - E_\gamma)t} \int d\vec{x} e^{-\frac{1}{\sigma_A} (\vec{x} - \vec{X}_A)^2 + i\vec{p}_\gamma \cdot \vec{x}} \\ &= N e^{i\Phi_0} \frac{2 \sin[(m_A - m_C - E_\gamma)T/2]}{(m_A - m_C - E_\gamma)} e^{-\frac{\sigma_A}{4} \vec{p}_\gamma^2}. \end{aligned} \quad (229)$$

In the above equation N and Φ_0 are constants. The square of the modulus of T is expressed in the form,

$$\int_0^T dt_1 dt_2 \frac{d\vec{p}_\gamma}{E_\gamma} e^{-i(m_A - m_C - E_\gamma)(t_1 - t_2)} e^{-\frac{\sigma_A}{2} \vec{p}_\gamma^2}, \quad (230)$$

where the integral

$$\int \frac{d\vec{p}_\gamma}{E_\gamma} e^{-i(m_A - m_C - E_\gamma)(t_1 - t_2)} e^{-\frac{\sigma_A}{2} \vec{p}_\gamma^2}, \quad (231)$$

is a smooth and short-range function of $t_1 - t_2$. Hence, the total probability is proportional to T and has no finite-size correction.

Particles in liquid are described also with wave packets and the probabilities of their reactions are studied in the same way.

5.2.3. *Decay in flight in dilute gas* . A photon has the effective mass in X-ray of γ -ray region in dilute gas and the rate is modified by the large finite-size correction. A radiative decay of A in flight in gas to C in flight and a photon γ , which have momenta, positions and wave packet sizes

$$\begin{aligned} A &: (E_A, \vec{p}_A, \sigma_A = \infty), \\ \gamma &: (\vec{X}_\gamma, E_\gamma, \vec{p}_\gamma, \sigma_\gamma), \\ C &: (E_C, \vec{p}_C, \sigma_C = \infty), \end{aligned} \quad (232)$$

is studied in a similar manner. Since $\sigma_A = \sigma_C = \infty$, the amplitude is expressed in the form of Eq. (218) with the effective mass of high-energy photon in X-ray or γ -ray regions, Eq. (175). The probability to detect this photon is given in Eq. (153) of the finite-size correction. The frequency that determines the finite-size correction for this photon of the energy E_γ is,

$$\omega = \frac{m_{eff}^2}{2E_\gamma}, \quad (233)$$

which gives a macroscopic distance.

5.3. Absorption

An absorption of γ is studied in a similar manner as the decay process. Process of A , C , and γ of the parameters,

$$\begin{aligned} A &: (\vec{X}_A, E_A, \vec{p}_A, \sigma_A), \\ \gamma &: (\vec{X}_\gamma, -E_\gamma, -\vec{p}_\gamma, \sigma_\gamma) \\ C &: (\vec{p}_C, E_C, \sigma_C), \end{aligned} \quad (234)$$

is described by replacing the sign of the photon's momentum in the previous amplitudes, Eq. (180) or Eq. (218). The distribution function deviates and central value of photon's energy $E_\gamma(\vec{p}_\gamma)$ becomes different from $E_A - E_C$ by the pseudo-Doppler effect, and the probability receives the large finite-size corrections in certain parameter regions.

6. Implications in particle decays

Implications of the probabilities modified by the finite-size correction or pseudo-Doppler effect are studied in decay experiments. The former correction depends on the mass, energy, life-time, and time-interval in the universal manner and its magnitude depends on the wave packet sizes and the internal structures. The effect of internal wave function to the light-cone singularity is analyzed in Appendix C and it is shown that for hadrons, nucleus, and positronium, the internal wave function does not modify the magnitude, but for atoms that is different. If the initial wave packets are small or $T \gg \tau$, the overlap of wave functions becomes negligible, whereas that becomes large if the initial wave packets are large and $T \leq \tau$. Especially the probability reveals various unusual behaviors for $\sigma_{initial} \gg \sigma_{final}$. The finite-size effect is easily observed directly with the measurements made with the detector located at various L . Conversely, the latter correction becomes large for the small wave packets, and the energy spectrum modified due to the pseudo-Doppler effect is easily observed with the detector if the energy resolutions and other properties of the detector are understood

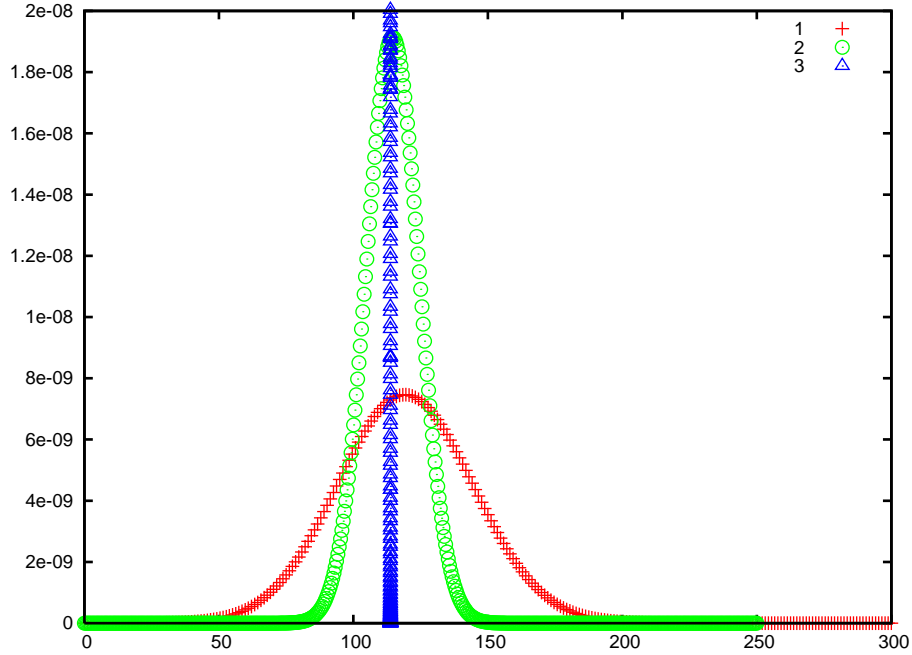


Fig. 5 The energy spectrum of gamma in J/Ψ decay at rest to $M(2981)$ and γ at $T = \infty$ is shown. The horizontal line shows the energy of γ in MeV for $\sigma_\gamma m_\pi^2 = 14.6, 100$, and ∞ , and the vertical line shows the probability. Wave packets of another daughter and parent are ∞ and $\sigma_{parent} m_\pi^2 = 10000$. The probability is the same for wide region of parent's wave packet. The spectrum is sharp for the plane wave and broad for the wave packets. The position of the peak shifts for the small wave packet due to pseudo-Doppler effect.

well. If they are unknown, the parameters of the detector are determined by comparing the theoretical values with the experimental data obtained from a standard sample. Calibration of the measuring apparatus may be used for this purpose.

We study various decay processes and present magnitudes of the finite-size and pseudo-Doppler effects for the parents of plane waves and the detecting particles of wave packets. Life-times of the parents are included, and spin independent components are studied.

6.1. Pseudo-Doppler effect

The energy spectrum is modified by the pseudo-Doppler effect in wide area and the distortion must be known not only for a precise analysis of experimental data but also for understanding physical phenomena. The comparison of the rates computed for plane waves, and wave packets of various sizes is given for $J/\Psi \rightarrow M(2981) + \gamma$ in Fig. (5). The total rates integrated over the final states agree but the energy spectra differ depending upon the wave packet size. The distributions and the shifts become wider and larger in smaller wave packets.

The broadening and shift of energies in other process such as $J/\Psi \rightarrow M(2981) + \gamma$, $J/\Psi \rightarrow \eta(1409) + \gamma$, $\pi \rightarrow \mu + \nu$, and $\mu \rightarrow e + \gamma$ are compared. They are sensitive to the wave packet size as in Figs. (6)-(8). Fig. (6) shows the variance of the final energy of various process. They are almost on one line. Hence, the wave packet size can be known from the variance of the energy of the final state. In Fig. (7), the normalized variance of energies of final states are presented. Those of heavy particle are different from those of light particle. In Fig.8, the

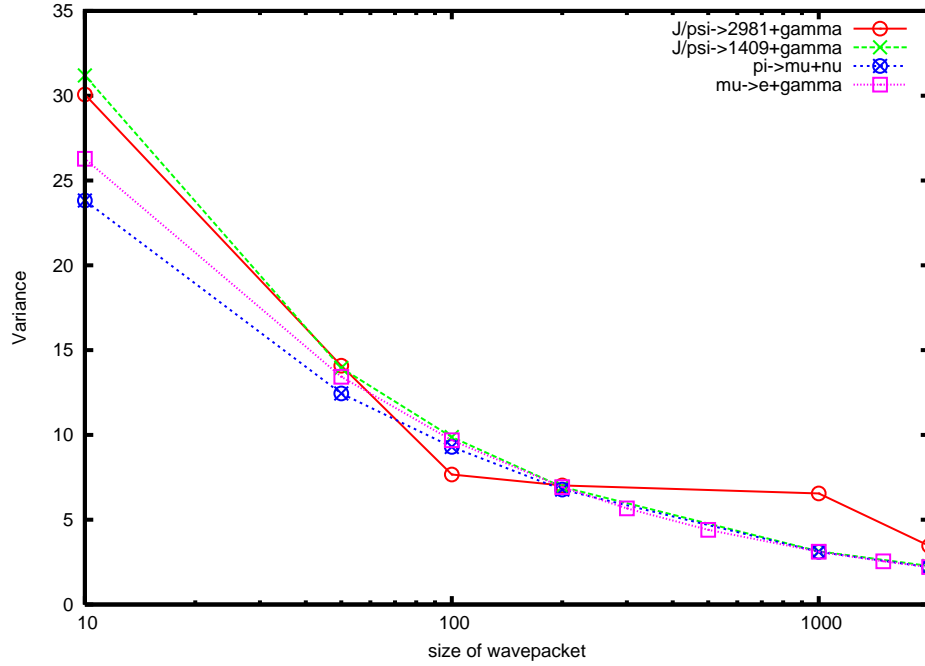


Fig. 6 The variance of final energy, $\Delta E = \sqrt{\langle (E_B + E_C)^2 \rangle - \langle E_B + E_C \rangle^2}$ in particle decays at rest measured at $T = \infty$ for $J/\Psi \rightarrow M(2981) + \gamma$ (red solid), $J/\Psi \rightarrow \eta(1409) + \gamma$ (green dot), $\pi \rightarrow \mu + \nu$ (blue dot), and $\mu \rightarrow e + \gamma$ (magenta dot). The horizontal line shows the size of wave packets in units of σm_π^2 and the vertical line shows the variance, ΔE . Wave packets of another daughter and parent are ∞ and $\sigma_{parent} m_\pi^2 = 10000$. Curves are almost on one line.

average energies of the final states are compared with the initial energies. The deviations are clearly seen, and the total energies of the final states become larger than those of the initial states.

6.1.1. Radiative transition of atom and positronium. An atom is a bound state of a nucleus and electrons and is heavy. Radiative transitions of atom, from an excited state to a lower energy-state, which emits a photon, are examples of the two body decays. Electrons bound to a nucleus have sizes of about 10^{-10} [m] and energies of about 10 [eV] or less. The photon is detected through its interaction with matter in a detector. Among various reactions, photo-electronic effect is the most important reaction, where an electron is emitted from the interacting photon with electrons. We assume here that the electron which the photon interacts with is a bound electron in atom at rest. The size of its wave function is about 10^{-10} [m]. So σ_γ has this size. For the initial particle A, σ_A has either about the same size, (1) 10^{-10} [m], for A in matter, or (2) larger than 10^{-10} [m], for A in vacuum or in dilute gas. In exceptional situation, (3) σ_A is smaller than 10^{-10} [m]. In experiments of $\delta E \approx |\delta \vec{p}|$

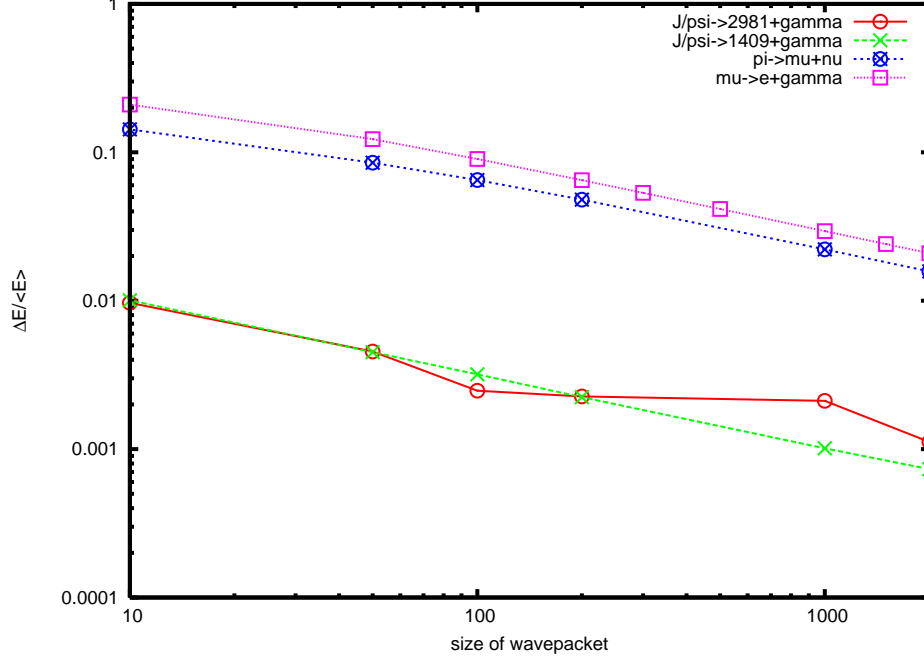


Fig. 7 The variance of energy of the final state over the average energy of the final state, $\Delta E/\langle E_B + E_C \rangle$ in particle decays at rest measured at $T = \infty$ for $J/\Psi \rightarrow M(2981) + \gamma$ (red solid), $J/\Psi \rightarrow \eta(1409) + \gamma$ (green dot), $\pi \rightarrow \mu + \nu$ (blue dot) and $\mu \rightarrow e + \gamma$ (magenta dot). The horizontal line shows the size of wave packets in units of σm_π^2 and the vertical line shows the deviations of the energies. Wave packets of another daughter and parent are ∞ and $\sigma_{parent} m_\pi^2 = 10000$. $\Delta E/\langle E_2 + E_3 \rangle$ is proportional to $(\sigma m_\pi^2)^{-1/2}$.

of the following three cases of the wave packet sizes,

- (1): $\sigma_A \approx \sigma_\gamma$,
- (2): $\sigma_A \gg \sigma_\gamma$,
- (3): $\sigma_A \ll \sigma_\gamma$,

the energy spectra are modified differently.

Positoronium is a bound state of an electron and its anti-particle, positron. Positoronium of positive charge conjugation decays to two gammas and that of negative charge conjugation decays to three gammas. The former is a second order QED process and the latter is a third order QED process, and the phase space are also different. Hence their decay rates are very different.

6.1.2. J/Ψ radiative decay. Photons produced in the decay

$$J/\Psi \rightarrow M + \gamma, \quad (235)$$

have energies in GeV region and may receive the pseudo-Doppler effect. The J/Ψ is produced in e^+e^- reaction and has a size determined with beam sizes, and meson M is detected with its decay products, which are stable hadrons such as pion, kaon and others. These charged

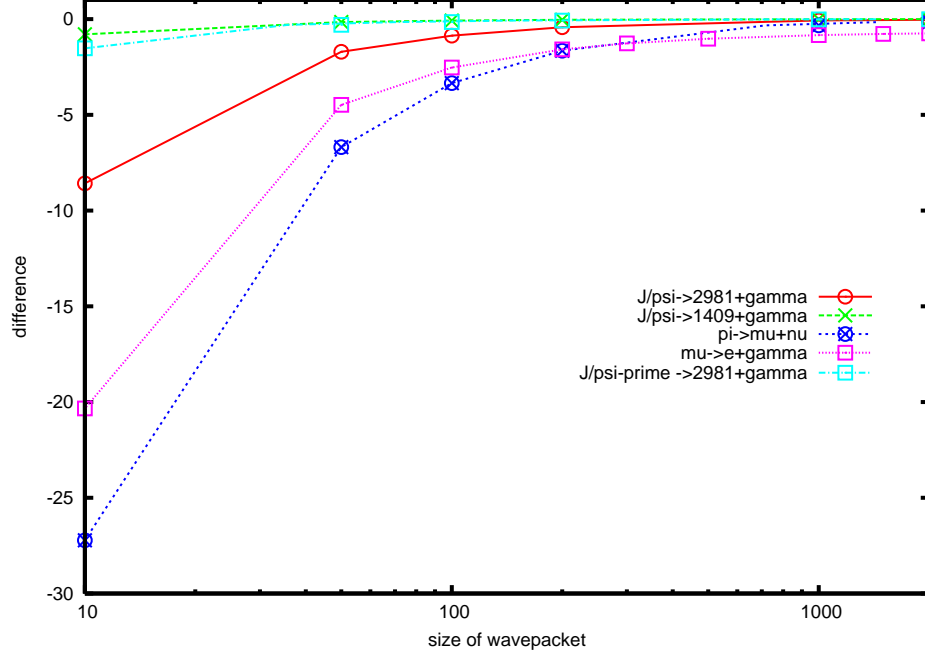


Fig. 8 The deviation of average energy of the final state from the initial mass, $m_A - \langle E_B + E_C \rangle$ [MeV], due to the pseudo-Doppler effect is given. There are finite deviations in various decays at rest measured at $T = \infty$ for $J/\Psi \rightarrow M(2981) + \gamma$ (red solid), $J/\Psi \rightarrow \eta(1409) + \gamma$ (green dot), $\pi \rightarrow \mu + \nu$ (blue dot), $\mu \rightarrow e + \gamma$ (magenta dot) and $\psi' \rightarrow M(2981) + \gamma$ (light-blue dot). The horizontal line shows the size of wave packets in units of σm_π^2 and the vertical line shows the deviations of the energies. Wave packets of another daughter and parent are ∞ and $\sigma_{parent} m_\pi^2 = 10000$.

particles have semi-microscopic sizes and σ_M has the same size. σ_γ is the order of the nuclear sizes.

These processes are important for QCD dynamics for $M = c\bar{c}$ state [36] or for glueball $M = \text{glue ball}$ [39]. Magnitudes of the corrections to the probabilities are not negligible as are presented in Figs. (6)-(8). The decay

$$\psi' \rightarrow M + \gamma, \quad (236)$$

is almost equivalent to Eq. (235) except the phase space and has smaller pseudo-Doppler effect due to large γ energy. Experiments show a difference between Eqs. (236) and (235) [37].

6.1.3. Two gamma decays of a heavy scalar particles. Positronium, neutral pion, charmonium P-states, and Higgs scalar decay to two photons. They are identified with reconstructed photon's energies and momenta. Detection of photons are made with photo-electric or Compton effects in low energy regions and with the e^-e^+ pair productions in high energies. The bound electrons of atoms in insulator have the size of 10^{-10} [m] so σ_γ for the former processes are of this size. The e^-e^+ pair is produced by an electric field around a heavy nucleus, which is short-range of nuclear size. Hence the wave packet size for the latter process is approximately the nuclear size in the high energy. Hence, the wave packets sizes of the gamma vary

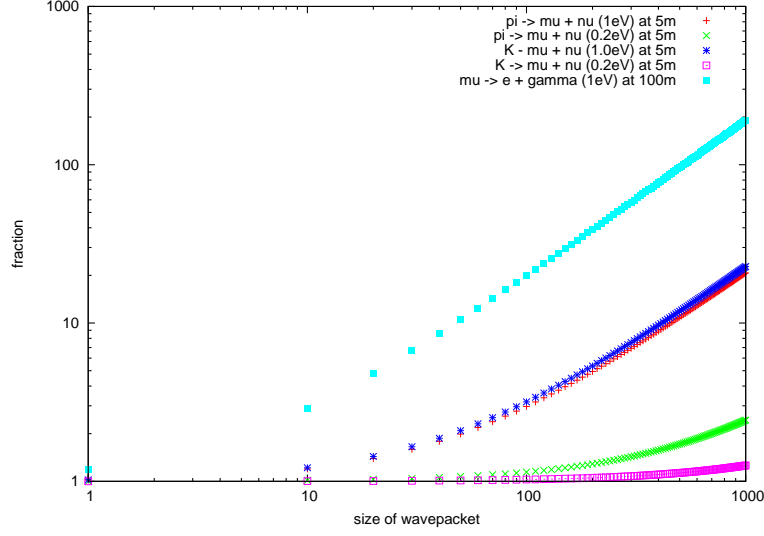


Fig. 9 The magnitudes of the probabilities in radiative and weak decays at rest measured at $T = 0.33 \times 10^{-6}(\mu)$, and $T = 1.7 \times 10^{-8}(\pi, K)$ [s] are shown. Parents and unobserved daughters are plane waves and observed particles are wave packets. The horizontal line shows the size of wave packets in units of σm_π^2 and the vertical line shows the enhancement factors at the finite distance, i.e., the ratios of the sum of the normal and diffraction components over the normal component. The decays of a pion to a muon and neutrino (red cross and green cross), and of a kaon to a muon and neutrino (blue-double cross and magenta box), and of a muon to an electron and photon (light-blue box) are presented. The masses are $m_\nu = 0.2$ and 0.5 [eV/c²], and $m_\gamma^{eff} = 1.0$ [eV/c²].

in wide range. They have short mean life times and pseudo-Doppler effects may appear in

$$M \rightarrow 2 \gamma. \quad (237)$$

6.2. Finite-size correction

The finite-size correction becomes large in the situation where the wave functions of the initial and final states overlap in wide area. This is realized at $T \leq \tau$ and is important in slow decays of particles, such as weak decays and some gamma decays. Fig. (9) shows the enhancement factors at the finite distance, i.e., ratios of the total probabilities over the normal probabilities of the asymptotic region in various weak and radiative decays. For the large wave packets, the values become large. In this figure, initial states are plane waves and size of wave packet for the neutrino is expressed in the units of $1/m_\pi^2$ and is written in the horizontal line. The ratios $\frac{P_{normal}+P_{diff}}{P_{normal}}$ are written in the vertical line. P_{diff} is large in the region $\sigma m_\pi^2 > 10$. Thus the finite-size corrections are non-negligible and important.

In the region $T \gg \tau$, the finite size corrections vanish, and the decay rates are expressed by the standard formula. In this region, the number of the parents decrease as $N_0 e^{-T/\tau}$ and that of the daughter becomes constant.

6.2.1. Slow gamma decays of Nucleus . Photons produced from radioactive nucleus are measured through their interactions with nucleus in targets which have finite sizes. Hence

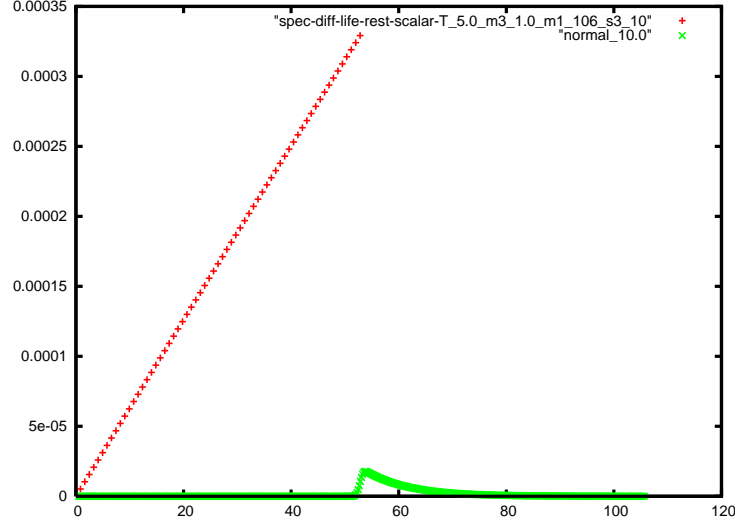


Fig. 10 The energy spectrum of photon in muon decays is shown at $T = 1.7 \times 10^{-8}$ [s] and $m_{\gamma}^{eff} = 1.0$ [eV/c²]. The horizontal line shows the energy of photon in MeV at $\sigma_{\gamma}m_{\pi}^2 = 100$, $\sigma_{\mu} = \sigma_e = \infty$ and the vertical line shows the probability. The normal component (green) has a sharp peak around 54 [MeV], and the diffraction component (red) spreads over wide region in the lower energy side and resembles the background.

$S[T]$ expressed by wave packets describe the amplitudes of the process,

$$N \rightarrow N' + \gamma. \quad (238)$$

From Appendix C, the magnitude of light-cone singularity and the diffraction component are almost equivalent to those of point particles, and the total probabilities are modified by P_{diff} .

6.2.2. Muon decay to an electron and gamma. A muon decays to an electron and a photon,

$$\mu \rightarrow e + \gamma, \quad (239)$$

where the photon's energy is about 50 [MeV], if the lepton number is violated. The lepton number violation has been observed in the neutrino oscillation phenomena but has not been in charged leptons. Precision measurements have been made and a new experiment has started [40]. Since the rate of this transition process is extremely small, it is important to know the corrections due to the pseudo-Doppler effect and finite-size correction. Those for the muon at rest of plane wave is studied here. From Fig. (6), the average energy of final state is larger than the initial energy.

Fig. (9) reveals the enhancement of the rates due to the diffraction for plane waves of muon and electron and the wave packet for gamma. Fig. (10) shows the energy spectrum of γ in the normal and diffraction components for $\sigma_{\gamma}m_{\pi}^2 = 100$, $\sigma_{\mu} = \sigma_e = \infty$ in the decay of muon of $\vec{p}_{\mu} = 0$ at $T = 1.7 \times 10^{-8}$ [s]. The normal component has a sharp peak around $E_{\gamma} \approx 54$ [MeV], whereas the diffraction component spreads over a wide region. Moreover the latter is much larger than the former in these parameters. Thus the corrections become important if the initial muon is a plane wave. The wave packet size of gamma can be

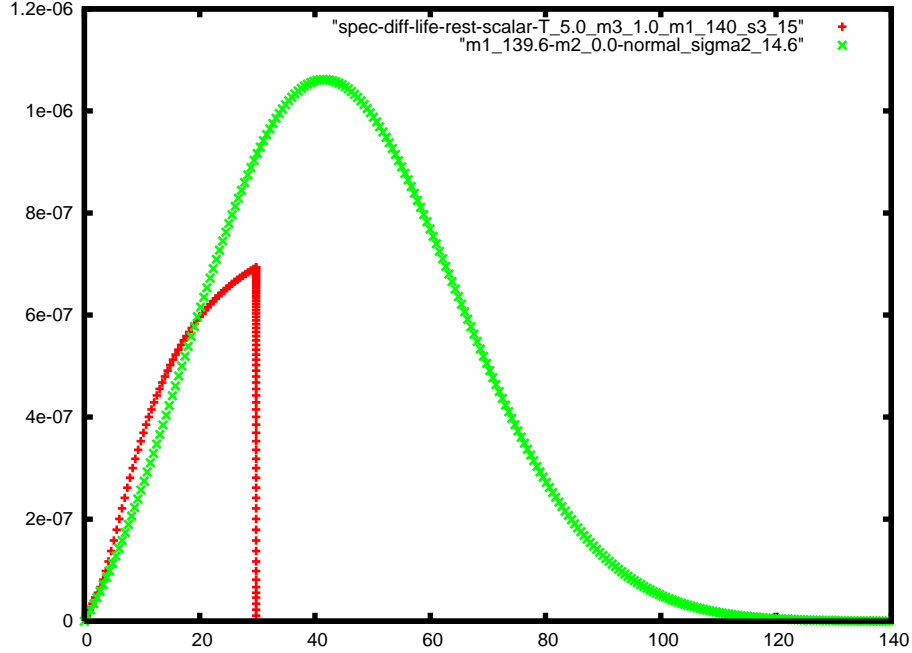


Fig. 11 The energy spectrum of neutrino in pion decay at rest at $T = 1.7 \times 10^{-8}$ [s] is shown. The horizontal line shows the energy in MeV at $\sigma_\nu m_\pi^2 = 14.6$, which corresponds ^{56}Fe and the vertical line shows the probability. Wave packets of another daughter and parent are ∞ and $\sigma_{parent} m_\pi^2 = 10000$. The neutrino mass is $m_\nu = 1.0$ [eV/ c^2]. The normal component (green) has a broad peak, and the diffraction component (red) spreads over in the low energy region.

determined from the spectrum at the higher energy region of a known process, and is used for the calculation of the diffraction component of the present process.

6.2.3. Weak decays . Neutrino measured through its interaction with a nucleus has a wave packet size of the nucleus. Hence the process of a nucleus

$$A \rightarrow A' + \nu, \quad (240)$$

is described by $S[T]$. The pion decay was discussed in the previous papers [41], and the neutrino's energy distribution is given in Fig.(11). From Appendix C, the magnitude of light-cone singularity and the diffraction component are about the same as point particles. The spectrum of diffraction component that gives the finite-size correction is distributed in the low energy region and that of the normal component is wide and has a peak. The peak is slightly shifted from that of the plane waves due to the pseudo-Doppler effect. From the shift and width of the normal component, the wave packet size can be determined and is used for the theoretical calculation of the diffraction component.

6.3. Proton decay

Proton is unstable and decays in Grand Unified Theory. In $SU(5)$ GUT, a main decay mode is

$$\text{proton} \rightarrow \pi^0 + e^+. \quad (241)$$

The initial proton is in matter in ground experiments and final states are detected through wave packets. For large wave functions of a proton, neutral pion, and positron, they overlap in a wide area. For small wave functions, they overlap in small area. General cases with the symmetric wave packets

$$\sigma_p, \sigma_{\pi^0}, \sigma_{e^+}, \quad (242)$$

of the four-dimensional momenta at positions

$$(p_p^0, \vec{p}_p; \vec{X}_p, T_p), (p_{\pi^0}^0, \vec{p}_{\pi^0}; \vec{X}_{\pi^0}, T_{\pi^0}), (p_{e^+}^0, \vec{p}_{e^+}; \vec{X}_{e^+}, T_{e^+}), \quad (243)$$

are studied in the following. They are governed by an interaction Lagrangian

$$\mathcal{L}_{int} = g\bar{\psi}_p(x)e(x)\varphi_\pi(x). \quad (244)$$

The transition amplitude is an integral over (t, \vec{x})

$$\begin{aligned} \mathcal{M}(p \rightarrow \pi^0 + e^+) &= g \int dt \int d\vec{x} e^{-\frac{1}{2\sigma_s}(\vec{x}-\vec{x}_0)^2 - \frac{1}{2\sigma_t}(t-t_0)^2} e^{R+i\phi} \tilde{\mathcal{M}}, \\ &= g(2\pi\sigma_s)^{\frac{3}{2}}(2\pi\sigma_t)^{\frac{1}{2}} e^{R+i\phi} \tilde{\mathcal{M}}, \end{aligned} \quad (245)$$

for finite values of σ_s and σ_t . $\tilde{\mathcal{M}}$ includes the spinors. σ_s and σ_t are given in the expressions

$$\frac{1}{\sigma_s} = \frac{1}{\sigma_p} + \frac{1}{\sigma_{\pi^0}} + \frac{1}{\sigma_{e^+}}, \quad (246)$$

$$\frac{1}{\sigma_t} = \frac{v_p^2}{\sigma_p} + \frac{v_{\pi^0}^2}{\sigma_{\pi^0}} + \frac{v_{e^+}^2}{\sigma_{e^+}} - \sigma_s \left(\frac{\vec{v}_p}{\sigma_p} + \frac{\vec{v}_{\pi^0}}{\sigma_{\pi^0}} + \frac{\vec{v}_{e^+}}{\sigma_{e^+}} \right)^2. \quad (247)$$

t_0 and $\vec{x}_0(t)$ are given in the form of Eq. (48) of an average velocity \vec{v}_0 ,

$$\vec{v}_0 = \sigma_s \left(\frac{\vec{v}_p}{\sigma_p} + \frac{\vec{v}_{\pi^0}}{\sigma_{\pi^0}} + \frac{\vec{v}_{e^+}}{\sigma_{e^+}} \right). \quad (248)$$

R and ϕ in the exponent are obtained from Eqs. (50), (51), and (53) as,

$$R = R_{\text{trajectory}} + R_{\text{momentum}}, \quad (249)$$

$$\begin{aligned} R_{\text{trajectory}} &= - \sum_j \frac{\tilde{X}_j^2}{2\sigma_j} + 2\sigma_s \left(\sum_j \frac{\tilde{X}_j}{2\sigma_j} \right)^2 + 2\sigma_t \left(\sum_j \frac{(\vec{v}_0 - \vec{v}_j) \cdot \tilde{X}_j}{2\sigma_j} \right)^2, \\ R_{\text{momentum}} &= - \frac{\sigma_t}{2} \left(E_p(\tilde{p}_p) - E_{\pi^0}(\tilde{p}_{\pi^0}) - E_{e^+}(\tilde{p}_{e^+}) \right)^2 - \frac{\sigma_s}{2} (\vec{p}_p - \vec{p}_{\pi^0} - \vec{p}_{e^+})^2, \end{aligned}$$

where

$$\tilde{p}_p = \vec{p}_p - \frac{\sigma_s}{\sigma_p} (\vec{p}_p - \vec{p}_{\pi^0} - \vec{p}_{e^+}), \quad (250)$$

$$\tilde{p}_{\pi^0} = \vec{p}_{\pi^0} + \frac{\sigma_s}{\sigma_{e^+}} (\vec{p}_p - \vec{p}_{\pi^0} - \vec{p}_{e^+}), \quad (251)$$

$$\tilde{p}_{e^+} = \vec{p}_{e^+} + \frac{\sigma_s}{\sigma_{e^+}} (\vec{p}_p - \vec{p}_{\pi^0} - \vec{p}_{e^+}), \quad (252)$$

and ϕ is a function of the momenta \vec{p}_j and positions \vec{X}_j .

1 Proton at rest

The proton in solid is at rest and is expressed with a small wave packet. In the rest system of the proton, the reduced momenta of Eq. (250) are

$$\tilde{\vec{p}}_p = \frac{\sigma_s}{\sigma_p}(\vec{p}_{\pi^0} + \vec{p}_{e^+}), \quad (253)$$

$$\tilde{\vec{p}}_{\pi^0} = \vec{p}_{\pi^0} - \frac{\sigma_s}{\sigma_{e^+}}(\vec{p}_{\pi^0} + \vec{p}_{e^+}), \quad (254)$$

$$\tilde{\vec{p}}_{e^+} = \vec{p}_{e^+} - \frac{\sigma_s}{\sigma_{e^+}}(\vec{p}_{\pi^0} + \vec{p}_{e^+}). \quad (255)$$

If the wave packet size of the positron is much larger than others

$$\sigma_{e^+} \gg \sigma_p, \sigma_{\pi^0}, \quad v_{e^+} \approx v_{\pi^0} \quad (256)$$

then,

$$\sigma_s = \frac{\sigma_p \sigma_{\pi^0}}{\sigma_p + \sigma_{\pi^0}}, \quad (257)$$

$$\begin{aligned} \frac{1}{\sigma_t} &= \frac{v_{\pi^0}^2}{\sigma_p + \sigma_{\pi^0}} + \frac{v_{e^+}^2}{\sigma_{e^+}} - \frac{2\sigma_p}{\sigma_{e^+}(\sigma_p + \sigma_{\pi^0})}(\vec{v}_{e^+} \cdot \vec{v}_{\pi^0}) \\ &\approx \frac{v_{\pi^0}^2}{\sigma_p + \sigma_{\pi^0}}, \end{aligned} \quad (258)$$

we have

$$\begin{aligned} R_{\text{momentum}} &= -\frac{\sigma_t}{2} \left(E_p(\tilde{\vec{p}}_p) - E_{\pi^0}(\tilde{\vec{p}}_{\pi^0}) - E_{e^+}(\tilde{\vec{p}}_{e^+}) \right)^2 - \frac{\sigma_s}{2} (\vec{p}_{\pi^0} + \vec{p}_{e^+})^2, \quad (259) \\ \tilde{\vec{p}}_p &= \frac{\sigma_s}{\sigma_p}(\vec{p}_{\pi^0} + \vec{p}_{e^+}), \quad \tilde{\vec{p}}_{\pi^0} = \vec{p}_{\pi^0}, \quad \tilde{\vec{p}}_{e^+} = \vec{p}_{e^+}. \end{aligned}$$

Thus in a region of large σ_s and σ_t , the conservation law of the momentum and energy are the same as that of plane waves, but in small σ_s the momenta are spread over in wide region and the energy conservation law is modified. For the large σ_t , in the event of

$$\vec{p}_{\pi^0} + \vec{p}_{e^+} \neq 0, \quad (260)$$

the energy conservation takes the form,

$$E_p(\tilde{\vec{p}}_p) - E_{\pi^0}(\tilde{\vec{p}}_{\pi^0}) - E_{e^+} \approx 0. \quad (261)$$

$\tilde{\vec{p}}_p$ could be very different from $\vec{p}_p = 0$, hence the modified conservation law derived from pseudo-Doppler effect should be taken into account for the experimental analysis in this region.

Since σ_t is finite, the decay probability is proportional to T in the region $T \ll \tau_{\text{proton}}$, and the decay rate is constant in a wide range of T despite the fact that the spectrum is distorted, where τ_{proton} is the average life-time. Thus the proton at rest decay with the constant rate even at small T and the proton decay experiment is doable if the life-time is less than $10^{34} - 10^{35}$ years.

6.3.1. Other decay processes . Three body decays such as $\mu \rightarrow e + \bar{\nu} + \nu$, $n \rightarrow p + e + \bar{\nu}$ and others have light particles in the final states and are modified by the pseudo-Doppler and finite-size corrections. They will be presented in a separate paper.

6.4. Thermodynamics of small quantum particles

When an excited state of heavy atom of the large wave packet size makes transition without changing the momentum and emit a photon, they follow the modified energy conservation law. If the atoms are in thermodynamic equilibrium of a temperature T , the state of the energy E follows a distribution

$$\rho(E, \beta) = N(-\beta E), \quad (262)$$

where β is inversely proportional to the temperature, and $N(-\beta E)$ becomes Planck distribution for Bosons and Fermi-Dirac distribution for Fermion.

In the situation where the wave packet size of the atoms is much larger than the wave packet size of a photon and the atoms are bound together strongly similar to Mössbauer effect, a distribution of the photon receives pseudo-Doppler effect and Mössbauer like effect. Then the temperature of photons becomes to deviate from that of the atoms.

From Eq. (57), in a situation

$$\sigma_\gamma \ll \sigma_A, \quad (263)$$

the velocity \vec{v}_0 agrees with the velocity of the photon. The photon's energy is given by Eq. (208), hence the energy distribution of the photon emitted from atoms is

$$\rho(E_\gamma, \beta) = N \frac{1}{e^{\tilde{\beta} E_\gamma} - 1}, \tilde{\beta} = \frac{\beta}{\kappa}. \quad (264)$$

Thus the effective temperature of the photon is κ times of that of the atoms.

7. Summary and implications.

We have developed a theory of the diffraction induced by many-body interactions and computed the finite-size corrections to the rates of slow transitions caused by electromagnetic and weak interactions. The large corrections to the Fermi's golden rule Eq. (13) were found in certain processes.

The Fermi's golden rule is applicable to the rates in the particle zone where the initial and final states separate completely and their wave functions do not overlap. The rates are not subject to $1/T$ correction. In the wave zone, however, the $1/T$ corrections are found using the wave functions that satisfy the boundary conditions. Because they have universal properties, they are observable in scattering experiments. The finite-size correction reveals the diffraction pattern of one quantum interference. The intermediate-time region of particle decays when the parent and daughters co-exit with a finite overlap of wave functions is the example of wave zone. The state is a superposition of the parent and daughters and has a finite expectation value of H_{int} . Thus the kinetic energy varies here, the decay rates and scattering cross sections are different from their asymptotic values.

The finite-size corrections are inevitable consequences of the boundary conditions at T and have the magnitude that depends on the sizes of σ_s . The size of σ_s can be controlled, and the finite-size corrections will be verified in experiments. Especially if the coherence length, $\hbar E/(m^2 c^3)$, is a macroscopic size much larger than de Broglie wave length $\hbar/|\vec{p}|$, they would reveal in macroscopic scales. For neutrinos or photon of the effective mass of the order $[eV/c^2]$, $\hbar E/(m^2 c^3)$ becomes a macroscopic size. Hence the finite-size correction may become visible in a macroscopic distance.

If $\sigma_s = \text{finite}$, $\sigma_t = \text{finite}$, the wave functions overlap only in microscopic regions. Waves in experiments at macroscopic distance are in the particle zone, and the finite-size correction disappears. Nevertheless, the probability receives pseudo-Doppler effect even in this region. The distortion of the energy distribution becomes stronger with smaller wave functions and may become visible. It becomes drastic if both of Mössbauer and pseudo-Doppler effects are combined as in Eq. (208). The final state of huge kinetic energy, much larger than the initial one, is formed with a small probability. The conservation of kinetic energy is violated in each event but satisfied for the average value over the classical time interval. Despite the fact that $S[\infty]$ conserves the kinetic energy, the modified energy $\delta\tilde{E}$ conserves approximately. In fact, these behaviors would have been considered as artifacts of the detectors and absorbed in calibrations of the detector. The present results might help toward the complete understanding in this direction.

In slow radiative and weak decays of particles A' and N' of plane waves,

$$A' \rightarrow A + \gamma, \quad N' \rightarrow N + \nu, \quad (265)$$

the rates and energy distributions of γ or ν in the asymptotic region,

$$\Gamma_{total} = \Gamma^{(0)}, \quad (266)$$

$$\mathcal{P}_{total}(E) = \mathcal{P}^{(0)}(E), \quad (267)$$

are computed with plane waves and $i\epsilon$ prescription, where E is the energy of the observed particle. Our results for γ or ν measured at L reveal the finite-size corrections and pseudo-Doppler effects and are expressed in the form,

$$\Gamma_{total} = \Gamma^{(n)} + \Gamma^{(diff)}(L; \sigma), \quad (268)$$

$$\mathcal{P}_{total}(E) = \mathcal{P}^{(n)}(E; \sigma) + \mathcal{P}^{(diff)}(L, E; \sigma). \quad (269)$$

The diffraction components have magnitudes summarized in Eqs. (154) and (178), and are important in various processes of leptons, hadrons, nucleus, and positronium and negligible in ordinary atoms. At $L \gg L_0$

$$\Gamma^{(diff)}(L; \sigma) \rightarrow 0, \quad (270)$$

$$\mathcal{P}^{(diff)}(L, E; \sigma) \rightarrow 0, \quad (271)$$

where L_0 is the minimum value of the mean length and coherence length,

$$L_0 = \min \left\{ c\tau, \frac{\hbar E}{m^2 c^3} \right\}. \quad (272)$$

As $\sigma \rightarrow 0$,

$$|\mathcal{P}^{(n)}(E; \sigma) - \mathcal{P}^{(0)}(E)| \rightarrow \text{large}, \quad (273)$$

$$\Gamma^{(diff)}(L; \sigma), \quad \mathcal{P}^{(diff)}(L, E; \sigma) \rightarrow 0, \quad (274)$$

whereas as $\sigma \rightarrow \text{large}$,

$$|\mathcal{P}^{(n)}(E; \sigma) - \mathcal{P}^{(0)}(E)| \rightarrow 0, \quad (275)$$

$$\Gamma^{(diff)}(L; \sigma), \quad \mathcal{P}^{(diff)}(L, E; \sigma) \rightarrow \text{large}. \quad (276)$$

The normal and diffraction components behave differently with σ , and Figs. (6) and (9) show them. From Eqs. (273) and (275), σ gives the effects to observables regardless of its magnitude

and can be determined experimentally from the energy spectrum Figs. (5)-(8) of the normal components $\mathcal{P}^{(n)}(E)$. The values computed by Fermi's golden rule have large corrections, Figs. (5)-(11), and the theoretical values can not be consistent with the experiments without corrections. Hence it would be easy to verify the finite-size corrections or pseudo-Doppler effect. Because the Fermi's golden rule is applied to many problems in wide area, it would be important to confirm the corrections.

The decay rate of proton in matter is constant in $T \ll \tau_{proton}$, if the final states are measured due to the boundary conditions. This agrees with the standard one, and the proton decay will be detected if GUT is correct. Finally unusual luminescence and thermodynamic properties of quantum particles caused by overlap of wave functions will be verified in experiments.

Constituent particles such as molecules, atoms, nucleus, or elementary particles have small intrinsic sizes and are expressed with wave functions of finite sizes in certain situations. Consequently, their reactions may be affected with finite-size corrections or pseudo-Doppler effects, even though any measurement are not made. Physical system may show such unusual behavior as the non-conservation of kinetic energy. Nevertheless the average energy over a long period recovers the conservation law. Hence the phenomena may appear in non-stationary and time-dependent processes. [33–35]. Macroscopic quantum phenomena in this situation have been barely studied and will be discussed in subsequent works.

Acknowledgements. The present work was partially supported by a Grant-in-Aid for Scientific Research(Grant No.24340043). The authors thank Drs. Kobayashi, Maruyama, Nakaya, Nishikawa, and Suekane for useful discussions on neutrino experiments, Drs. Asai, Kinoshita, Kobayashi, Minowa, Mori, Nio, Yamada for useful discussions on interferences, Drs. Sato, Sorai, Takesada, and Watanabe for useful discussions on wide physical phenomena.

References

- [1] H. Lehman, K. Symanzik, and W. Zimmermann, *Nuovo Cimento.* **1**, 1425 (1955).
- [2] F. Low, *Phys. Rev.* **97**, 1392 (1955).
- [3] M. L. Goldberger and Kenneth M. Watson, *Collision Theory* (John Wiley & Sons, Inc. New York, 1965).
- [4] R. G. Newton, *Scattering Theory of Waves and Particles* (Springer-Verlag, New York, 1982).
- [5] J. R. Taylor, *Scattering Theory: The Quantum Theory of non-relativistic Collisions* (Dover Publications, New York, 2006).
- [6] M. Gell-Mann, “The Quark and the Jaguar: Adventures in the Simple and the Complex”, St. Martin's Griffin; ILL edition(1995). This book illuminated us.
- [7] R. G. Winter, *Phys. Rev.* **123**, 1503 (1961).
- [8] M. L. Goldberger and K. M. Watson, *Phys. Rev.* **136**, 1472 (1964).
- [9] H. Ekstein and A. J. F. Siegert, *Ann. Phys.* **68**, 509 (1971).
- [10] K. J. F. Gaemers and T. D. Visser, *Physica.* **A 153**, 234 (1988).
- [11] A. Einstein, B. Podolsky, and N. Rosen, *Phys. Rev.* **47**, 777 (1935).
- [12] L. Schiff, “Quantum Mechanics”, page 197, McGRAW-HILL, New-York. L. D. Landau and E. M. Lifshitz, “Quantum Mechanics”, page 157, Butterworth Heine Mann, New York, (2003).
- [13] P. A. M. Dirac, *Proc. R. Soc. Lond.* **A114**, 243 (1927).
- [14] Von V. Weisskopf and E. Wigner, *Zeit Phys.* **63**, 54 (1930).
- [15] L. I. Schiff, *Quantum Mechanics* (McGRAW-Hill Book COMPANY, Inc. New York, 1955).
- [16] See for instance, M. Peshkin, “Quantum Field Theory”, Sect. 7.2, page 222, McGRAW-HILL, New-York; S. Weinberg, “The Quantum Theory of Fields I”, page 109, Cambridge University, Cambridge; M. Srednicki, “Quantum Field Theory, page 37, Cambridge University press, Cambridge, 2007. The complete set of wave packets is constructed with those that have centers of position and momentum in [17] and used.
- [17] K. Ishikawa and T. Shimomura, *Prog. Theor. Phys.* **114**, 1201 (2005) [hep-ph/0508303].
- [18] K. Ishikawa and Y. Tobita, arXiv:1106.4968 [hep-ph].
- [19] K. Ishikawa and Y. Tobita, arXiv:1109.3105 [hep-ph].
- [20] K. Ishikawa and Y. Tobita, *Prog. Theor. Phys.* **122**, 1111 (2009) [arXiv:0906.3938 [quant-ph]].

-
- [21] K. Ishikawa and Y. Tobita, [arXiv:0801.3124]; “Neutrino mass and mixing” in the 10th Inter. Symp. on “Origin of Matter and Evolution of Galaxies” AIP Conf. proc. 1016, 329 (2008).
- [22] B. Kayser, Phys. Rev. **D24**, 110(1981); Nucl. Phys. **B19** (Proc.Suppl), 177 (1991).
- [23] C. Giunti, C. W. Kim, and U. W. Lee, Phys. Rev. **D44**, 3635 (1991)
- [24] S. Nussinov, Phys. Lett. **B63**, 201 (1976).
- [25] K. Kiers, S. Nussinov and N. Weiss, Phys. Rev. **D53**, 537 (1996) [hep-ph/9506271].
- [26] L. Stodolsky, Phys. Rev. **D58**, 036006 (1998) [hep-ph/9802387].
- [27] M. Beuthe, Phys. rept. **375**, 105 (2003) [arXiv:hep-ph/0109119].
- [28] H. J. Lipkin, Phys. Lett. **B642**, 366 (2006) [hep-ph/0505141].
- [29] E. K. Akhmedov, JHEP. **0709**, 116 (2007) [arXiv:0706.1216 [hep-ph]].
- [30] A. Asahara, K. Ishikawa, T. Shimomura, and T. Yabuki, Prog. Theor. Phys. **113**, 385 (2005) [hep-ph/0406141]; T. Yabuki and K. Ishikawa, Prog. Theor. Phys. **108**, 347 (2002).
- [31] A. H. Mueller, Phys. Rev. **D12**, 2963 (1970).
- [32] K. Wilson, in Proceedings of the Fifth International Symposium on Electron and Photon Interactions at High Energies, Ithaca, New York, 1971, 115 (1971); See also N. N. Bogoliubov and D. V. Shirkov, *Introduction to the Theory of Quantized Fields* (John Wiley & Sons, Inc. New York, 1976).
- [33] David J. Flannigan and Kenneth S. Suslick, Nature **434** 7029, 52 (2005); B. P. Barber and Seth J. Putterman, Phys. Rev. Lett. **69**, 3839 (1992).
- [34] C. G. Camara, et al, Nature, **455**, 1089 (2008).
- [35] See for example, H. Tsuchiya, et al, Phys. Rev. Lett. **99**, 165002 (2007); A. Chilingarian, et al, Phys. Rev. **D82**, 043009 (2010); T. Torii, et al, Geo. res. Lett. **38**, L24801 (2011); M. Tavani, et al, Phys. Rev. Lett. **106**, 018501 (2011).
- [36] See part of Charmonium in Ref. [38].
- [37] See for instance, J. E. Gaiser, SLAC-255, UC-34D (1982).
- [38] J. Beringer, *et al.* [Particle Data Group], Phys. Rev. **D86**, 010001 (2012).
- [39] K. Ishikawa, Phys. Rev. Lett. **46**, 978 (1981); Chanowitz, Phy. Rev. Lett. **46**, 981 (1981); See also particle data summary on $\eta(1409)$ [38].
- [40] J. Adam, et al, arXiv:1303.0754 [hep-ex].
- [41] K. Ishikawa and Y. Tobita, arXiv:1206.2593 [hep-ph]; arXiv:1209.5585 [hep-ph]; arXiv:1209.5586 [hep-ph].

Appendix A. Finite-size correction to Fermi’s golden rule

A-I. Approximation with Dirac’s delta function

Integrals over the finite interval

$$\int_0^T dt e^{i\omega t} = e^{i\omega T/2} \frac{\sin(\omega T/2)}{\omega/2}, \quad (\text{A1})$$

$$\int_0^T dt_1 dt_2 e^{i\omega(t_1-t_2)} = \left(\frac{\sin(\omega T/2)}{\omega/2} \right)^2, \quad (\text{A2})$$

are approximated normally with

$$\int_0^T dt e^{i\omega t} = 2\pi\delta(\omega), \quad (\text{A3})$$

$$\int_0^T dt_1 dt_2 e^{i\omega(t_1-t_2)} = 2\pi T\delta(\omega), \quad (\text{A4})$$

for a large T. They have been applied in computing a decay rate and cross section and are explained in most textbooks.

Finite-size correction to this formula depends on ω . If ω is discrete,

$$\int_0^T dt e^{i\omega t} = \begin{cases} T; & \omega = 0, \\ \frac{2 \sin(\omega T/2)}{\omega} e^{i\omega T/2}; & \omega \neq 0, \end{cases} \quad (\text{A5})$$

$$\int_0^T dt_1 dt_2 e^{i\omega(t_1-t_2)} = \begin{cases} T^2; & \omega = 0, \\ \left(\frac{2 \sin(\omega T/2)}{\omega} \right)^2; & \omega \neq 0, \end{cases} \quad (\text{A6})$$

and the averages over finite time interval δT of $\delta T \omega \gg 1$ are

$$\text{Aver} \left[\int_0^T dt e^{i\omega t} \right] = \begin{cases} T; & \omega = 0, \\ \frac{i}{\omega}; & \omega \neq 0, \end{cases} \quad (\text{A7})$$

$$\text{Aver} \left[\int_0^T dt_1 dt_2 e^{i\omega(t_1-t_2)} \right] = \begin{cases} T^2; & \omega = 0, \\ \frac{2}{\omega^2}; & \omega \neq 0. \end{cases} \quad (\text{A8})$$

For the average probability at a finite- T , the correction is given by

$$\frac{2}{\omega^2 T^2}. \quad (\text{A9})$$

A-II. Correction by Taylor expansion

If ω is continuous, there exists states of infinitesimal energy differences. The correction becomes non-trivial and is studied here. The following integral for $\omega_1 < 0 < \omega_2$

$$I(\omega_1, \omega_2; T) = \int_{\omega_1}^{\omega_2} d\omega g(\omega) \left(\frac{\sin(\omega T/2)}{\omega} \right)^2, \quad (\text{A10})$$

coincides with $2\pi T g(0)$ if the second equation of Eq. (A3) is used. To find next order terms in $1/T$, we expand $g(\omega)$

$$g(\omega) = g(0) + \sum_{l=1}^{\infty} \frac{g^{(l)}(0)}{l!} \omega^l, \quad (\text{A11})$$

and change the variable to $x = \omega T$,

$$\begin{aligned} I(\omega_1, \omega_2; T) &= T \int_{\omega_1 T}^{\omega_2 T} dx \left(\frac{\sin(x/2)}{x} \right)^2 g(x/T) \\ &= \sum_l \frac{g^{(l)}(0)}{l! T^{l-1}} \int_{\omega_1 T}^{\omega_2 T} dx \left(\frac{\sin(x/2)}{x} \right)^2 x^l. \end{aligned} \quad (\text{A12})$$

The integrand in the above equation is finite at $x = 0$ for $l = 0$, but those for $l \geq 1$ vanish. At large x , $\sin^2(x/2) \approx 1/2$. So we have

$$\begin{aligned} I(\omega_1, \omega_2; T) &\approx 2\pi T g(0) + \sum_{l \geq 1} \frac{g^{(l)}(0)}{l! T^{l-1}} \int_{\omega_1 T}^{\omega_2 T} dx x^l \frac{1}{x^2} \frac{1}{2} \\ &= 2\pi T g(0) + \frac{g^{(1)}(0)}{2} \log \left| \frac{\omega_2}{\omega_1} \right| + \sum_{l \geq 2} \frac{g^{(l)}(0)}{2l!} \frac{(\omega_2^{l-1} - \omega_1^{l-1})}{l-1}. \end{aligned} \quad (\text{A13})$$

Choosing $\omega_1 = -\omega_2$, we have

$$I(-\omega_2, \omega_2; T) = 2\pi T g(0) + \sum_{l \geq 1} \frac{g^{(l+1)}(0)}{2(l+1)!} \frac{1}{l} (\omega_2^l (1 - (-)^l)), \quad (\text{A14})$$

The second term in the above equation is the $1/T$ correction. This correction depends on the cut off frequencies and the constant term i.e., ω_2^0 term vanishes at the symmetric cut off $\omega_1 = -\omega_2$. So $\lim_{\omega_2 \rightarrow 0} I(-\omega_2, \omega_2; T)$ agrees with $2\pi T g(0)$. The finite-size correction is written in the form,

$$I(-\omega_2, \omega_2; T) = 2\pi T g(0) \left(1 + \frac{T_0}{T} \right), \quad (\text{A15})$$

where T_0 is roughly estimated with a size of atom as

$$T_0 = \frac{10^{-10} [\text{m}]}{c} = 0.3 \times 10^{-18} [\text{s}], \quad (\text{A16})$$

in atomic physics. Hence in an experiment of the size $1 [\text{m}]$, $T = 1/c = 0.3 \times 10^{-8} [\text{s}]$, and the correction becomes

$$\frac{T_0}{T} = 10^{-10}. \quad (\text{A17})$$

This value is negligible and the finite-size correction vanishes at a macroscopic distance.

Appendix B. Level density and correlation function :quantum mechanics

We summarize the probability at a finite T , Eq. (11), of systems of various level densities. When a level density $\rho(E)$ is given, a number of states below E , s , satisfies

$$\frac{ds}{dE} = \rho(E). \quad (\text{B1})$$

The correlation function is expressed with s in the form,

$$g^{(+)}(t_1 - t_2) = \int_{E_0}^{\infty} dE \rho(E) e^{i(E-E_0)(t_1-t_2)} = \int_0^{\infty} ds e^{i(E(s)-E_0)(t_1-t_2)}, \quad (\text{B2})$$

$$g^{(-)}(t_1 - t_2) = \int_{E_m}^{E_0} dE \rho(E) e^{i(E-E_0)(t_1-t_2)} = \int_{s_m}^0 ds e^{i(E(s)-E_0)(t_1-t_2)}. \quad (\text{B3})$$

Using s , we have the integral over a finite interval of s of Eq. (A3), $C(T) = I(0, \infty, T)$,

$$\begin{aligned} C(T) &= \int_0^T dt_1 dt_2 g(t_1 - t_2) = \int_{s_1}^{s_2} ds \int_0^T dt_1 dt_2 e^{i\omega(s)(t_1-t_2)}, \\ \omega(s) &= E(s) - E_0, \quad g(t_1 - t_2) = g^{(+)}(t_1 - t_2) + g^{(-)}(t_1 - t_2), \end{aligned} \quad (\text{B4})$$

which agrees with

$$= 2\pi T \int_{s_1}^{s_2} ds \delta(\omega(s)) = 2\pi T \frac{1}{|\omega'(s_0)|} = 2\pi T \rho(E_0), \quad (\text{B5})$$

if $\omega(s) = 0$ has a simple root, s_0 in $s_1 < s_0 < s_2$ and $\omega'(s_0)$ is not too small. This is equivalent to Eq. (A3). $C(T)$ is written also in the expression

$$C(T) = T \int_{-T}^T d\xi g(\xi) + \int_{-T}^0 d\xi \xi g(\xi) - \int_0^T d\xi \xi g(\xi). \quad (\text{B6})$$

B-I. Regular level density

For the level densities that are regular at $E = E_0$,

$$\rho(E) = c_0, \frac{1}{E - E_0 - i\Gamma}, e^{-c|E-E_0|^2}, \quad (\text{B7})$$

we have

Table B1

$\rho(E)$	s	$g(t_1 - t_2)$	$C(T)$
c_0	$c_0(E - E_0)$	$2\pi c_0 \delta(t_1 - t_2)$	$2\pi c_0 T$
$\frac{1}{E - E_0 - i\Gamma}$	$\int_{E_0}^E \frac{dE'}{E' - E_0 - i\Gamma}$	$e^{-\Gamma(t_1 - t_2)}$	$\frac{2T}{\Gamma} \left(1 - \frac{1 - e^{\Gamma T}}{\Gamma T} \right)$
$e^{-c E-E_0 }$	$\int_{E_0}^E dE' e^{-c E'-E_0 ^2}$	$e^{-\frac{(t_1 - t_2)^2}{2c}}$	$\sqrt{\frac{c\pi}{2}} \left(T - \sqrt{\frac{8c}{\pi}} \right)$

The correlation functions $g(t_1 - t_2)$ in Table B1 are short range and Eq. (A3) is applicable. $C(T)$ are proportional to T and the corrections are proportional to $1/T$.

B-II. Weakly singular level density

For the level densities,

Table B2

$\rho(E)$	$\rho(0)$	$\rho'(0)$	s	$g(t_1 - t_2)$	$C(T)$
$e^{-C E-E_0 }$	1	\pm	$C \int_{E_0}^E dE' e^{-C E'-E_0 }$	$\frac{1}{C - i(t_1 - t_2)}$	$\left(T\pi - 2C \log \frac{T}{C} \right)$
$C(E - E_0)^p$ ($0 < p < 1$)	0	∞	$\frac{C(E - E_0)^{p+1}}{p+1}$	$\frac{\Gamma(\frac{p+1}{2})2^{p-\frac{1}{2}}}{\Gamma(-\frac{p}{2}) t_1 - t_2 ^{p+1}}$	$T \times \infty$

The correlation functions $g(t_1 - t_2)$ are long range and Eq. (A3) is applicable in the first one but is not in the second one. $C(T)$ are proportional to T and the correction is proportional to $(\log T)/T$ in the former one and the proportional constant diverges in the latter one. Especially in the latter case, the level density satisfies, $\rho(E_0) = 0$, but the coefficient $C(T)/T$ diverges.

B-III. Singular level density

For the singular level densities

Thus Eq. (A3) is not applicable in the level densities of Table B3. The level density satisfies $\rho(E_0) = \infty$ and decay rates $C(T)/T$ is proportional to a positive power of T . Thus this system should reveals unusual non-Markov property.

Table B3

$\rho(E)$	$\rho(0)$	$\rho'(0)$	s	$g(t_1 - t_2)$	$C(T)$
$C\delta(E - E_0)$	∞	∞	$C\theta(E - E_0)$	C	CT^2
$\frac{C}{ E - E_0 ^p}; 0 < p < 1$	∞	∞	$\frac{C(E - E_0)^{1-p}}{1-p}$	$C\sqrt{\frac{2}{\pi}} \frac{p\pi\Gamma(1-p)}{2 t_1 - t_2 ^{1-p}}$	$\frac{2T^{1+p}}{p}$

B-IV. Relativistic wave packet

The spectrum density $\rho(\omega)$ for a two-body decay $A \rightarrow B + C$ of relativistic particles Eq. (128) integrated over \vec{p}_C is

$$\rho(\omega) = \int \frac{d\vec{p}_C}{(2\pi)^3} e^{-\sigma_B(\vec{p}_A - \vec{p}_B - \vec{p}_C)^2} \delta(\omega - E_A(\vec{p}_A) + E_C(\vec{p}_C) + E_B(\vec{p}_A - \vec{p}_C)). \quad (B8)$$

$\rho(0)$ is finite because the root of $\omega = 0$ exists and $\rho(\omega)$ satisfies

$$\rho(\omega) = \begin{cases} 0, & \omega > E_A, \\ e^{-\frac{\sigma_B}{4}\omega^2}, & \omega \rightarrow -\infty. \end{cases} \quad (B9)$$

Due to smooth asymptotic behavior Eq. (B9), the following integral converges even at a finite T ,

$$\int d\omega \left(\frac{\sin(\omega T/2)}{\omega} \right)^2 \rho(\omega) = T \left(2\rho(0) \int dx \left(\frac{\sin x}{x} \right)^2 + \frac{1}{T} \eta \right), \quad (B10)$$

where η is given by

$$\eta = \int d\omega \left(\frac{\sin(\omega T/2)}{\omega} \right)^2 \tilde{\rho}(\omega) > 0, \quad \tilde{\rho}(\omega) = \rho(\omega) - \rho(0), \quad (B11)$$

and the positivity Eq. (35) is fulfilled.

Appendix C. Light-cone singularity for general composite systems

C-I. Light-cone singularity and form factor

Composite particles such as hadrons, nucleus, atoms, and molecules have internal structures and have modified light-cone singularities. The form factor $F((p_A - p_C)^2)$ in

$$\langle C; \vec{p}_C | J(x) | A; \vec{p}_A \rangle = e^{-i(p_A - p_C) \cdot x} \Gamma F((p_A - p_C)^2), \quad (C1)$$

depends on Lorenz scalar $(p_A - p_C)^2$, where $J(x)$ is source operator of γ , ν , or others that are detected. Lorentz indices are ignored. The correlation function is

$$\begin{aligned} \Delta_{A,C}(\delta x) &= \frac{1}{(2\pi)^3} \int \frac{d\vec{p}_C}{E(\vec{p}_C)} |F((p_A - p_C)^2)|^2 G(p_A, p_C) e^{-i(p_A - p_C) \cdot \delta x} \\ &= G(p_A, -i \frac{\partial}{\partial \delta x} - p_A) \frac{1}{(2\pi)^3} \int \frac{d\vec{p}_C}{E(\vec{p}_C)} |F((p_A - p_C)^2)|^2 e^{-i(p_A - p_C) \cdot \delta x}, \\ G(p_A, p_C) &= \sum (\Gamma \Gamma^*)_{A,C}, \end{aligned} \quad (C2)$$

and we have the light-cone singularity,

$$\begin{aligned}
& \frac{1}{(2\pi)^3} \int \frac{d\vec{p}_C}{E(\vec{p}_C)} |F((p_A - p_C)^2)|^2 e^{-i(p_A - p_C) \cdot \delta x} \\
&= \frac{2}{i\pi(2\pi)^3} \int d^4q \text{Im} \left[\frac{1}{q^2 + m_A^2 - m_C^2 + 2p_A \cdot q - i\epsilon} \right] |F(q^2)|^2 e^{-iq \cdot \delta x} \\
&= |F(m_C^2 - m_A^2)|^2 \left(\frac{i}{2\pi} \delta(\lambda) \epsilon(\delta t) + \text{"others"} \right). \tag{C3}
\end{aligned}$$

Thus we have

$$\Delta_{A,C}(\delta x) = G(p_A, -i \frac{\partial}{\partial \delta x} - p_A) |F(m_C^2 - m_A^2)|^2 \left(\frac{i}{2\pi} \delta(\lambda) \epsilon(\delta t) + \text{"others"} \right).$$

The magnitude is renormalized by the form factor $|F(m_C^2 - m_A^2)|^2$ and the form is kept intact.

C-II. Strength

$|F(m_C^2 - m_A^2)|^2$ of various systems, using the energy gap, ΔE , and size, R ,

$$m_A = m_C + \delta E, \quad F(q^2) = F(0) e^{-\frac{R}{2} \sqrt{-q^2}}, \tag{C4}$$

is written as

$$F(m_C^2 - m_A^2)^2 = F(0)^2 e^{-R\sqrt{2m_C\delta E}}, \tag{C5}$$

and is determined by $R\sqrt{2m_C\delta E}$.

The typical values for bound states composed of electron, nucleon, quark, and μ -on, eA , e^+e^- , NN , $q\bar{q}$, qqq , μN , μ^+e^- , and $e(K)A$ are

$$R = \begin{cases} \frac{\hbar c}{m_e c^2} \frac{1}{\alpha}; & (\text{atom: } eA), \\ 2 \frac{\hbar c}{m_e c^2} \frac{1}{\alpha}; & (\text{positronium: } e^+e^-), \\ \frac{\hbar}{m_\pi c}; & (\text{nucleus: } NN), \\ \frac{\hbar}{m_q c}; & (\text{hadron: } q\bar{q}, qqq), \\ \frac{\hbar c}{m_\mu c^2} \frac{1}{\alpha}; & (\mu \text{ atom: } \mu A), \\ \frac{\hbar c}{m_e c^2} \frac{1}{\alpha}; & (\mu \text{ atom: } \mu e), \\ \frac{\hbar c}{m_e c^2} \frac{1}{N_K \alpha}; & (\text{K-shell atom: } eA), \end{cases} \quad \Delta E = \begin{cases} \frac{m_e c^2 \alpha^2}{2}; & (\text{atom: } eA), \\ \frac{m_e c^2 \alpha^2}{2}; & (\text{positronium: } e^+e^-), \\ \frac{m_\pi c^2}{100}; & (\text{nucleus: } NN), \\ m_q c^2; & (\text{hadron: } q\bar{q}, qqq), \\ \frac{m_\mu c^2 \alpha^2}{2}; & (\mu \text{ atom: } \mu A), \\ \frac{m_e c^2 \alpha^2}{2}; & (\mu \text{ atom: } \mu e), \\ \frac{m_e c^2 \alpha^2}{2}; & (\text{K-shell atom: } eA), \end{cases} \tag{C6}$$

and,

$$m_C = \begin{cases} m_N; \text{ (atom: } eA), \\ 2m_e; \text{ (positronium : } e^+e^-), \\ Am_N; \text{ (nucleus : } NN), \\ Bm_qc^2; \text{ (hadron : } q\bar{q}, qq), \\ m_N; \text{ (}\mu \text{ atom: } \mu A), \\ m_\mu; \text{ (}\mu \text{ atom: } \mu e), \\ m_N; \text{ (K-shell atom: } eA). \end{cases} \quad (\text{C7})$$

We have

$$\frac{R}{\hbar} \sqrt{2m_c \Delta E} = \begin{cases} \sqrt{\frac{\hbar^2 c^2}{m_e^2 c^4 \alpha^2} m_N \frac{m_e c^2 \alpha^2}{\hbar^2 2}} = \sqrt{\frac{m_N}{m_e}} \geq 50; \text{ (atom: } eA), \\ \sqrt{\frac{m_e}{m_e}} = 1; \text{ (positronium : } e^+e^-), \\ \sqrt{\frac{Am_N}{100m_\pi}} \leq 1; \text{ (light nucleus),} \\ \approx 3 (A = 100); \text{ (nucleus : } NN), \\ \sqrt{B} \approx 1; \text{ (hadron : } q\bar{q}, qq), \\ \sqrt{\frac{m_N}{m_\mu}} = 3; \text{ (}\mu \text{ atom: } \mu A), \\ \sqrt{\frac{m_\mu}{m_e}} = 14; \text{ (}\mu \text{ atom: } \mu e), \\ \sqrt{\frac{m_N}{N_K m_e}} = 10; \text{ (K-shell atom: } eA), \end{cases} \quad (\text{C8})$$

and

$$F(m_C^2 - m_A^2)^2 = \begin{cases} F(0)^2 \times O(1); \text{ hadron, positronium, light nucleus,} \\ F(0)^2 \times O(10^{-1}); \text{ } \mu N\text{-atom, heavy nucleus,} \\ F(0)^2 \times O(10^{-5}); \text{ } \mu e\text{-atom, K-electron,} \\ F(0)^2 \times O(10^{-10}); \text{ atom.} \end{cases} \quad (\text{C9})$$

Thus the magnitude of light-cone singularity is about 1 of $F(0)^2$ for positronium, light nucleus, and hadrons, and 10^{-1} for μN -atom and heavy nucleus, and 10^{-5} for μe -atom and K-electron, and 10^{-10} for atom. Atom is composed of heavy nucleus and electrons and its size and energy gap are determined by electron's mass. Hence the large ratio $\sqrt{m_N/m_e}$ determines the overlap of an atom C with an atom A , and the strength of the light-cone singularity becomes extremely weak, accordingly. For other particles composed of equal masses, $F(m_C^2 - m_A^2) \approx F(0)$.